ASTROBIOLOGY
Volume 14, Number 6, 2014

DOI: 10.1089/ast.2013.1122

Production and Early Preservation of Lipid Biomarkers in Iron Hot Springs

Mary N. Parenteau,[1,2] Linda L. Jahnke,[2] Jack D. Farmer,[3] and Sherry L. Cady[4,5]

Abstract

The bicarbonate-buffered anoxic vent waters at Chocolate Pots hot springs in Yellowstone National Park are 51–54°C, pH 5.5–6.0, and are very high in dissolved Fe(II) at 5.8–5.9 mg/L. The aqueous Fe(II) is oxidized by a combination of biotic and abiotic mechanisms and precipitated as primary siliceous nanophase iron oxyhydroxides (ferrihydrite). Four distinct prokaryotic photosynthetic microbial mat types grow on top of these iron deposits. Lipids were used to characterize the community composition of the microbial mats, link source organisms to geologically significant biomarkers, and investigate how iron mineralization degrades the lipid signature of the community. The phospholipid and glycolipid fatty acid profiles of the highest-temperature mats indicate that they are dominated by cyanobacteria and green nonsulfur filamentous anoxygenic phototrophs (FAPs). Diagnostic lipid biomarkers of the cyanobacteria include midchain branched mono- and dimethylalkanes and, most notably, 2-methylbacteriohopanepolyol. Diagnostic lipid biomarkers of the FAPs (*Chloroflexus* and *Roseiflexus* spp.) include wax esters and a long-chain tri-unsaturated alkene. Surprisingly, the lipid biomarkers resisted the earliest stages of microbial degradation and diagenesis to survive in the iron oxides beneath the mats. Understanding the potential of particular sedimentary environments to capture and preserve fossil biosignatures is of vital importance in the selection of the best landing sites for future astrobiological missions to Mars. This study explores the nature of organic degradation processes in moderately thermal Fe(II)-rich groundwater springs—environmental conditions that have been previously identified as highly relevant for Mars exploration. Key Words: Lipid biomarkers—Photosynthesis—Iron—Hot springs—Mars. Astrobiology 14, 502–521.

1. Introduction

1.1. Biogeochemistry of iron hot springs

Terrestrial hydrothermal systems have long been recognized as habitats for microbial life on Earth (Brock, 1967, 1978; Castenholz, 1969). The composition of the hydrothermal fluids, which dictate which microbial populations are present, is controlled by a complex set of interactions between the magmatic gases, the deep parent brine, mineral dissolution of the wall rock, deposition of secondary minerals, underground boiling, vapor loss, dilution, and mixing with fluids of different origin (Giggenbach, 1988). In general, the rhyolite and basalt-hosted hydrothermal systems in Yellowstone National Park are characterized by two geochemically distinct end members: (1) alkaline-chloride silica-depositing hot springs and (2) acid-sulfate boiling pools, mud pots, and fumaroles (Fournier, 1989). Mixing of these two geochemical end members generates a spectrum of acid-sulfate-chloride (ASC) springs (Fournier, 1989). Depending on the host rock and pH, some of these ASC springs can be high in iron.

The ASC waters at Chocolate Pots hot springs, ~5 km southwest of Norris Geyser Basin, are pH 5.5–6.0, 51–54°C, and contain 5.8–5.9 mg/L dissolved Fe(II) (Pierson *et al.,* 1999; Pierson and Parenteau, 2000; Trouwborst *et al.,* 2007; Parenteau and Cady, 2010). As a result of buffering by high levels of bicarbonate (Parenteau and Cady, 2010), the vent waters are slightly acidic, which allows the Fe(II) to remain in solution. The pH is also just above the lower limit for prokaryotic phototrophs such as cyanobacteria, which do not tolerate pH values below ~4.5 (Castenholz, 1988). This pH range allows cyanobacteria and green nonsulfur filamentous anoxygenic phototrophs (FAPs) (*e.g.*, *Chloroflexus* and

[1]SETI Institute, Mountain View, California.
[2]NASA Ames Research Center, Exobiology Branch, Moffett Field, California.
[3]School of Earth and Space Exploration, Arizona State University, Tempe, Arizona.
[4]Department of Geology, Portland State University, Portland, Oregon.
[5]Pacific Northwest National Laboratory, Richland, Washington.
Frances Westall (Centre de Biophysique Moléculaire, CNRS, Orléans, France) served as guest editor and made editorial decisions for this manuscript.

Roseiflexus spp.) to grow in the presence of high levels of Fe(II). To better understand the evolution of oxygenic photosynthesis, our group studied the physiological ecology of this ecosystem and searched for cyanobacteria that use Fe(II) as an electron donor for photosynthesis (Pierson *et al.,* 1999). We have also quantified the impact of cyanobacterial oxygen production on Fe(II) oxidation as a model for Precambrian Fe(II) oxidation (Trouwborst *et al.,* 2007).

1.2. Biosignatures in hot springs

We are currently examining the production and early preservation of microbial biosignatures (biofabrics, microfossils, and lipid biomarkers) by iron oxides in this system. The preservation of microbial biosignatures in terrestrial hot springs via the rapid entombment of the microbes by aqueous mineral precipitates was identified long ago as relevant to understanding the processes of microbial fossilization on early Earth and Mars (*e.g.,* Walter, 1972; Walter and Des Marais, 1993; Farmer, 1995; Cady and Farmer, 1996; Farmer and Des Marais, 1999; Cady *et al.,* 2003; Farmer, 2003). Most studies have been directed toward elucidating the mechanisms of silica permineralization in microbial fossil preservation (*e.g.,* Cady and Farmer, 1996; Farmer 1999; Phoenix *et al.,* 2000; Konhauser *et al.,* 2001; Mountain *et al.,* 2003; Benning *et al.,* 2004; Ferris and Magalhaes, 2008), one of the common modes of microfossil preservation in Precambrian cherts (*e.g.,* Walsh and Lowe, 1985). There have also been studies that examined the production and preservation of microbial lipids in modern and subrecent siliceous sinters that have not undergone significant diagenesis (Jahnke *et al.,* 2001, 2004; Pancost *et al.,* 2005, 2006; Talbot *et al.,* 2005; Gibson *et al.,* 2008; Kaur *et al.,* 2008, 2011).

In contrast to the silicification studies, preservation of microbial biosignatures by iron oxides is relatively understudied because it is generally thought that iron-rich sediments do not preserve biosignatures well (*e.g.,* Klein, 2005). However, our previous studies have revealed excellent early preservation of cyanobacterial microfossils by nanophase iron oxyhydroxide (ferrihydrite) permineralization (Parenteau and Cady, 2010) and distinct dendritic microbial biofabrics by iron encrustation (Wade *et al.,* 1999; Parenteau and Cady, 2010). Other groups have reported preservation of microfossils by nanophase iron oxides in modern as well as ancient settings in the Río Tinto acid mine drainage system (Fernández-Remolar *et al.,* 2005; Fernández-Remolar and Knoll, 2008), which is more acidic than the Chocolate Pots system.

Examining the capture and retention of microbial biosignatures in modern hot springs is relevant to the search for evidence of past microbial life in analogous deposits on Mars. Hydrothermal activity on Mars is supported by evidence for widespread volcanism and higher heat flow during the Noachian (4.1–3.7 Ga) (*e.g.,* Farmer, 1996; Baratoux *et al.,* 2011). This is supported by the recent discovery of siliceous hydrothermal deposits by the Spirit rover at Home Plate in the Columbia Hills, Gusev Crater, Mars (Ruff *et al.,* 2011). The subsurface could have provided a major habitat for thermophilic life, and warm mineralizing surface springs could have provided optimal conditions for fossil biosignature capture and preservation (Walter and Des Marais, 1993; Farmer and Des Marais, 1999). Chocolate Pots hot springs, which is a surface expression of moderately thermal, slightly acidic Fe(II)-rich groundwater, provides a site at which to study the taphonomy of organic compounds in iron-silica systems and provides useful insights for evaluating the preservation potential of iron-rich sedimentary rocks on Mars.

This study focused on the characterization of lipid biomarkers in the modern iron-mineralized, prokaryotic phototrophic mats in this understudied class of bicarbonate-buffered ASC iron hot springs. Specifically, we used lipid biomarkers to (1) describe the community composition of four types of phototrophic mats and (2) determine how lithification by siliceous 2-line ferrihydrite, the primary iron oxide phase of the sinter, affects the biomarker signature of the communities. The aim was to characterize the taphonomy of the lipid biomarkers in this iron-rich system, namely, which compounds survive microbial degradative processes within the mats and through the earliest stages of diagenesis in the iron deposits beneath the mats. We also examined the survival of organics in a nearby extinct iron-silica spring that has undergone significant postdepositional cementation during diagenesis.

2. Methods

2.1. Field measurements

The temperature and pH of the water that flows over the microbial mats at Chocolate Pots hot springs were measured as described in Parenteau and Cady (2010). The dissolved Fe(II) concentration was measured by using the colorimetric ferrozine assay with a Hach DR/2400 portable spectrophotometer (Pierson *et al.,* 1999; Parenteau and Cady, 2010). Detailed chemical analyses of the thermal waters have been performed several times since 1935; the last two samplings

Table 1. Geochemical Composition of Vent Waters at Chocolate Pots Hot Springs

Species (mg/L)	*Pierson and Parenteau, 2000*	*Parenteau and Cady, 2010*
Temperature (°C)	52.5	51.8
pH	5.9	5.7
Aluminum	0.17	0.1
Ammonium nitrogen	< 0.1	nd
Bicarbonate	248	nd
Boron	nd	0.5
Calcium	20	21
Carbonate	0	nd
Chloride	28	29
Fluorine	nd	4.5
Iron(II)	5.1	5.5
Iron(III)	< 0.1	nd
Total iron	nd	5.4
Lithium	nd	0.8
Magnesium	3	2.0
Manganese	1.04	1.4
Nitrate nitrogen	< 0.2	nd
Nitrite nitrogen	< 0.2	nd
Potassium	24	23
Phosphorous	0.01	< 0.1
Silica	159	141
Sodium	102	115
Sulfate	32	25
Sulfide	0	nd

nd, not determined.

are summarized in Table 1 (Pierson and Parenteau, 2000; Parenteau and Cady, 2010).

2.2. Sample collection

Four distinct phototrophic mat types were identified in previous studies of the *in situ* physiological ecology of this system (Pierson *et al.,* 1999; Pierson and Parenteau, 2000), including (1) *Synechococcus*-Chloroflexi, (2) *Pseudanabaena* spp., (3) *Oscillatoria* cf. *princeps*, and (4) narrow *Oscillatoria* spp. The phylum-level designation of Chloroflexi is used to include the green nonsulfur FAPs *Chloroflexus* and *Roseiflexus*, both of which are present in the *Synechococcus*-Chloroflexi mat. These mat systems, which are briefly reviewed below, provided a focus for the lipid biomarker study reported here.

The *Synechococcus*-Chloroflexi mat and the *Pseudanabaena* mat were located closest to the vents and consequently experienced the highest temperature and levels of Fe(II) (Figs. 1 and 2a, 2d, Table 2). The *Oscillatoria princeps* mat occurred in areas of low flow and was associated with a floating reflective mineral/organic film that broke into fragments when handled (Fig. 2e, Table 2). The fourth mat type, narrow *Oscillatoria*, was the most widely distributed over the iron spring deposits and occurred as two types of mat morphologies: terracette structures on the steep face of the main iron deposit (Figs. 1 and 2c, Table 2) and laminated mats in a rapidly flowing channel (Figs. 1 and 2b, Table 2). These mats were collected in July 2003 and immediately placed on dry ice in the field. Frozen samples were stored on dry ice during transit to the laboratory, where they were subsequently freeze-dried. Freeze-dried samples were stored at 4°C until lipid analyses were performed in August 2003.

To characterize the preservation of lipids in the iron oxide sinter, a 1 cm × 2.5 cm deep core of the *Synechococcus*-Chloroflexi mat was removed, frozen, and sectioned with a sterile scalpel into two parts: (1) the top 2 mm of mat and a thin layer (~ 0.5 mm) of the iron oxide sinter beneath the mat, and (2) the remaining underlying 2.5–25 mm iron oxide sinter. The maximum core depth was dictated by the conditions of our National Park Service research permit. A

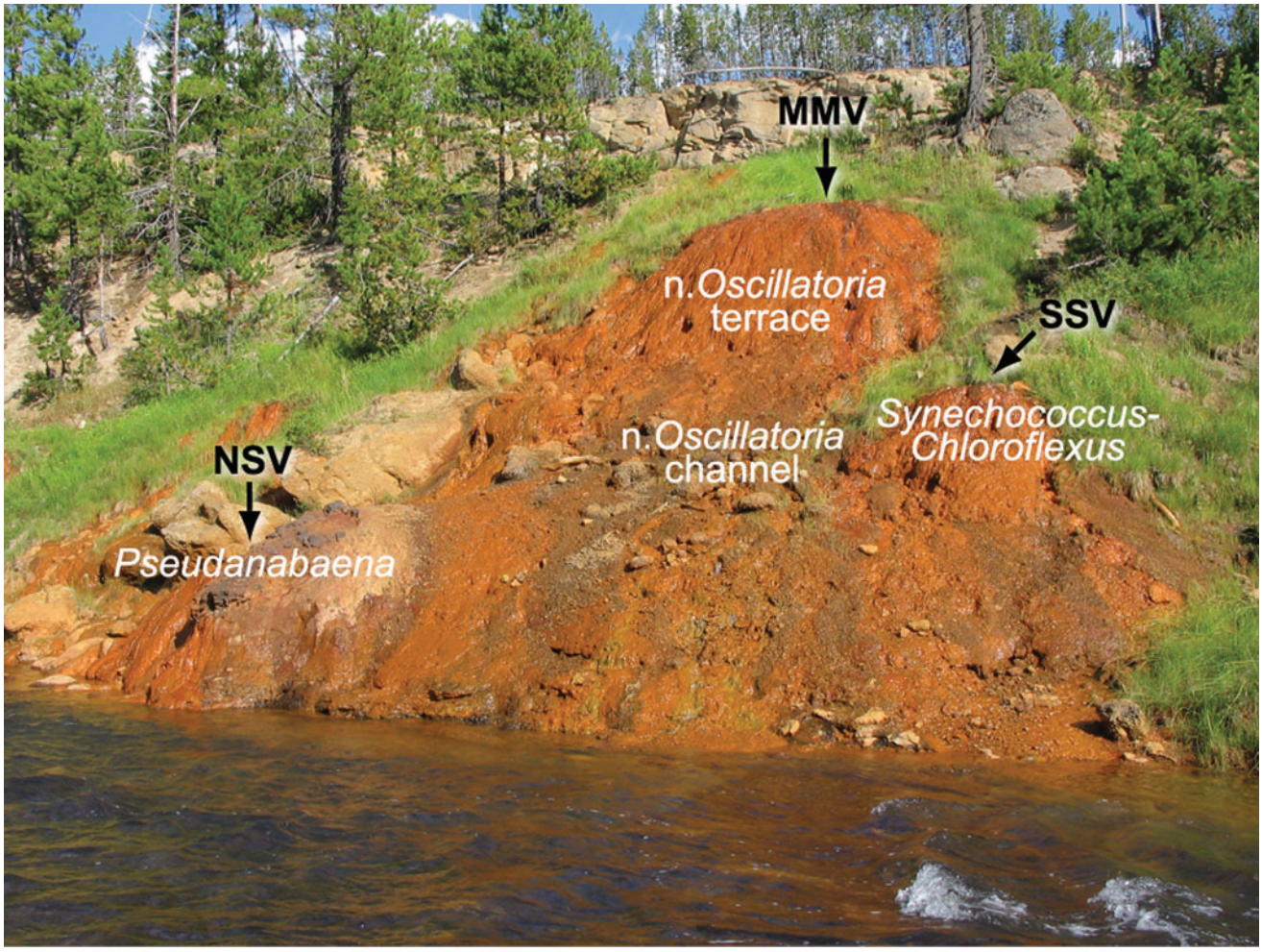

FIG. 1. Distribution of three phototrophic mats examined in this study on the main Chocolate Pots iron deposit. The *Pseudanabaena* mat occurred at the north satellite vent (NSV). The narrow *Oscillatoria* mat occurred in a terracette structure on the steep face of the main iron deposit and in the rapidly flowing vent outflow channel. The *Synechococcus*-Chloroflexi mat occurred at the south satellite vent (SSV). The *Oscillatoria princeps* mat occurred in areas of low flow (not pictured). MMV, main mound vent.

TABLE 2. GEOCHEMICAL MEASUREMENTS OF PHOTOTROPHIC MATS AT CHOCOLATE POTS HOT SPRINGS

Sample	*Temperature (°C)*	*pH*	*Fe(II) (mg/L)*	*% TOC*
Synechococcus-Chloroflexi mat core (a)	52.8	5.9	5.9	1.3
Ferrihydrite beneath mat (b)	52.8	5.9	5.9	0.2
Ferrihydrite core adjacent to mat	51.5	6.0	5.9	0.3
Pseudanabaena mat	50.4	5.5	5.8	28.8
Oscillatoria cf. *princeps* mat	41.4	5.8	nd	11.6
Narrow *Oscillatoria* mat terrace	40.1	7.3	0.4*	0.4
Narrow *Oscillatoria* mat channel	39.6	7.3	0.2*	2.2

nd, not determined.
*Measured above mat types in 2005.

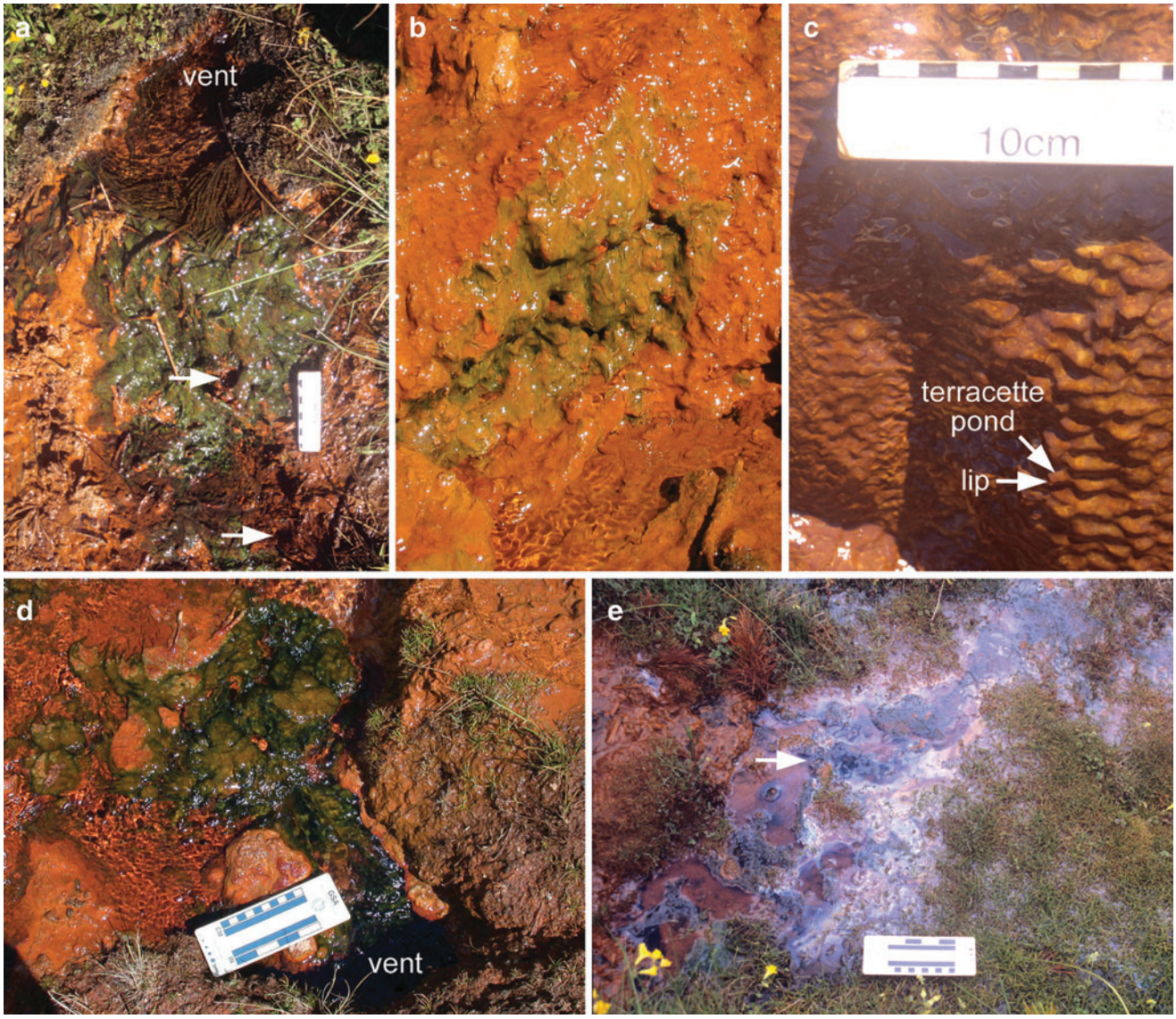

FIG. 2. Field images of the four phototrophic mats examined in this study. (**a**) The *Synechococcus*-Chloroflexi mat in the vent pool. A core of the mat was removed (upper arrow) and sectioned into the mat, and ferrihydrite beneath the mat. A ferrihydrite core with no conspicuous mat on the surface was also collected (lower arrow). (**b**) Narrow *Oscillatoria* mat in rapid outflow channel. (**c**) Narrow *Oscillatoria* mat in association with a terracette structure on the steep face of the main iron deposit. (**d**) Floating streams of the *Pseudanabaena* mat near the north satellite vent. (**e**) The *Oscillatoria princeps* mat (arrow) in association with reflective iron film that fractured upon handling.

similar-size core of iron oxide sinter with no conspicuous mat on the surface was also collected adjacent to the *Synechococcus*-Chloroflexi mat core site. All the samples were immediately placed on dry ice in the field, freeze-dried in the laboratory, and analyzed within a month of returning them to the lab, as noted above.

A hand sample of fossilized microbial ''streamer'' fabric (*i.e.,* centimeter-scale tufts of microbes oriented in the direction of water flow) was removed from an extinct iron-silica spring deposit located approximately 700 m north of Chocolate Pots (Fig. 3). The outcrop of sinter was exposed in a cut bank along the Gibbon River. Petrographic thin sections were prepared from the sinter block with the streamer fabric oriented in cross section, or perpendicular to the bedding. Light micrographs were acquired with a Nikon Microphot FXA microscope. Epifluorescence images of the immature kerogen in the microfossils were acquired by using a blue excitation filter (420–490 nm).

2.3. Elemental analysis and X-ray diffraction

The freeze-dried phototrophic mats and iron oxide sinter samples were analyzed for total carbon and total organic carbon (TOC) as previously described (Parenteau and Cady, 2010). The extracted mat and iron oxide cores were prepared for powder X-ray diffraction (XRD) as previously described (Parenteau and Cady, 2010). XRD patterns of the extinct iron-silica sinter were obtained with Terra, which is a terrestrial analogue of the CheMin instrument on the Mars Science Laboratory Curiosity rover (Sarrazin *et al.,* 2008). Terra and CheMin are combination XRD/XRF instruments designed for rock and mineral analysis in the field and on

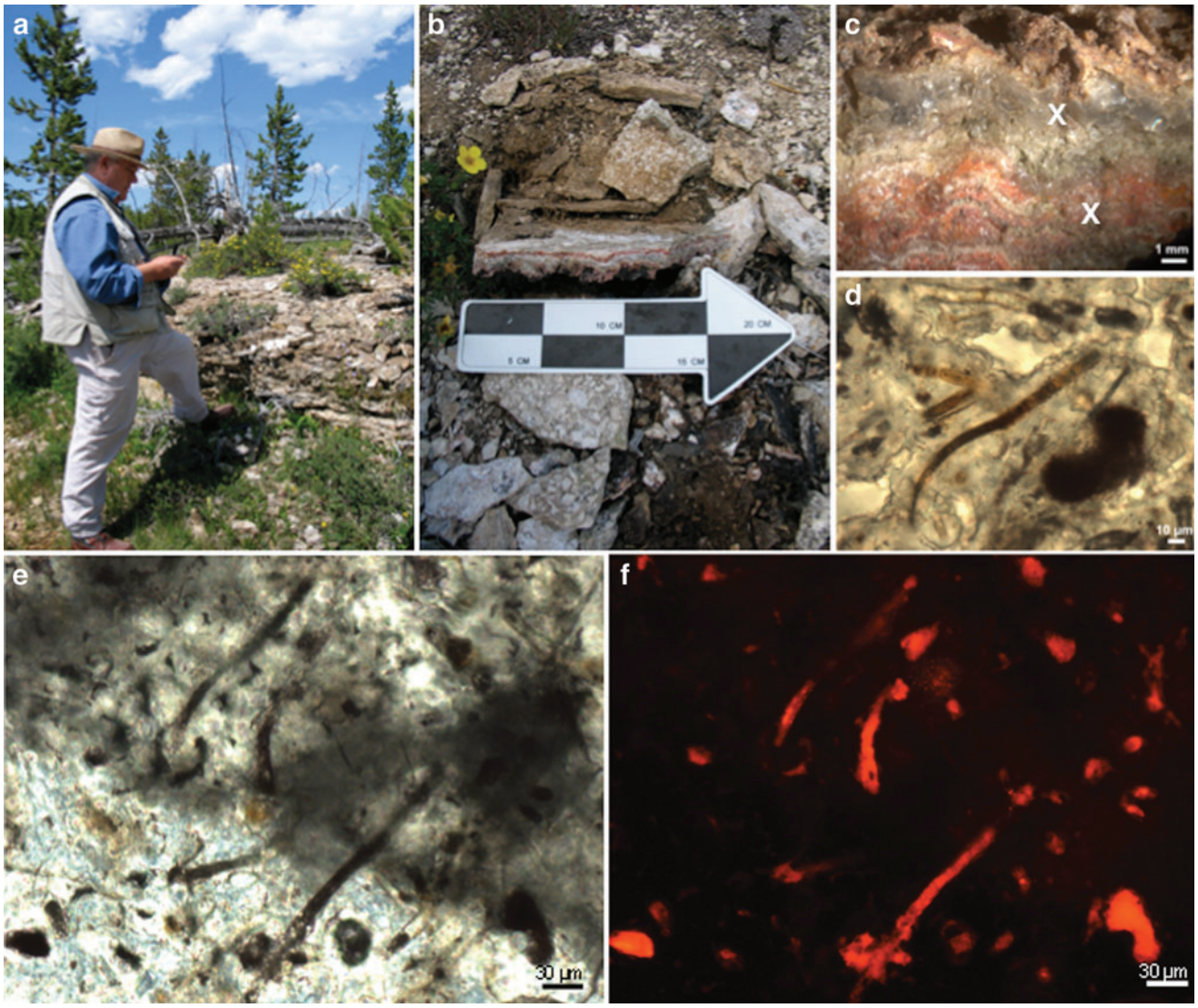

FIG. 3. Field images and micrographs of the extinct iron-silica hot spring located approximately 700 m north of Chocolate Pots. (**a**) Outcrop of sinter. (**b**) End-on view of a hand sample of a fossilized streamer biofabric. (**c**) End-on view of biofabric viewed under a dissecting microscope. Streamers present in iron band on top of sample. Underneath are alternating laminae of opaline silica (upper X) and iron (lower X). (**d**) Remarkably well-preserved *Calothrix* filament. Amber-colored kerogen visible in microfossils. (**e**) More filamentous microfossils in a matrix of silica and iron. (**f**) Same field of view as in (e), revealing the fluorescence of immature kerogen in the microfossils and dispersed throughout the biofabric.

Mars, respectively. The peaks on the powder XRD patterns were identified by comparing the measured sample d-spacings to previously published iron oxide and opal-A d-spacings.

2.4. Lipid extraction, separation, and derivatization

Lipids were extracted with a modified Bligh and Dyer procedure (Jahnke *et al.,* 1992) to generate a total lipid extract. Phosphatidylcholine (Sigma) was added as an internal extraction standard, and the total lipid extract was separated into polar and neutral fractions by using a cold acetone precipitation. The polar lipid precipitate was separated into glycolipids, phospholipids, and bacteriohopanepolyols (BHPs) by preparative thin-layer chromatography (TLC) on Silica gel G plates (Merck) with the use of an acetone-benzene-water (91:30:8) solvent system (Pohl *et al.,* 1970). The Sigma standards digalactosyl diglyceride (DG) and phosphatidylglycerol (PG) were used to aid in the identification of the glycolipid and phospholipid zones, respectively. The BHPs were recovered from the spotting zone ($R_f = 0$).

The neutral lipids (acetone supernatant) were separated into hydrocarbons, wax esters, pigments, and glycolipids by preparative TLC on Silica gel G plates (Merck) by subsequent development in methylene chloride and then hexane (Jahnke *et al.,* 2004). The Sigma standards C_{14}–C_{25} *n*-alkane mix ($R_f = 0.95$), hexadecyl hexadecanoate ($R_f = 0.8$), and cholestanol ($R_f = 0.2$) were used to identify hydrocarbon, wax ester, and pigment/glycolipid zones, respectively. The (bacterio)chlorophylls and glycolipids were recovered from the lower portion of the plate ($R_f = 0$ to ~ 0.2).

The polar fractions (polar glycolipids, phospholipids, and BHPs) and the neutral fractions (pigments and neutral glycolipids) were recovered from the TLC plates by eluting with the Bligh and Dyer procedure. The polar glycolipids, phospholipids, pigments, and neutral glycolipids were treated by using a mild alkaline methanolysis procedure, which generates fatty acid methyl esters (FAMEs) and chlorophyll-derived phytol (Jahnke *et al.,* 2001, 2004). The bond position of the monounsaturated FAMEs was determined by preparing dimethyl disulfide (DMDS) adducts (Yamamoto *et al.,* 1991). In the case of the phospholipid fraction from the iron sinter cores, the sample size was not sufficient, and the proportion of Δ9 and Δ11 $C_{18:1}$ was determined by retention times relative to methyl ester standards of palmitoleic acid ($C_{18:1\Delta9}$) and vaccenic acid ($C_{18:1\Delta11}$). Hopanols (C_{31}, C_{32} and 2-methylhomologs) were prepared by treatment of the BHPs with an oxidation-reduction procedure and were analyzed as acetate derivatives (Rohmer *et al.,* 1984; Jahnke *et al.,* 2004). Phytol was hydrogenated prior to gas chromatography analysis (Jahnke *et al.,* 2004). For characterization of *Chloroflexus* fatty acid double-bond positions, the type strain *Chloroflexus aurantiacus* J-10-fl was obtained from Beverly Pierson (Professor Emerita, University of Puget Sound) and grown photoheterotrophically at 50°C (Pierson and Castenholz, 1974).

2.5. Gas chromatography

Fatty acid methyl esters, DMDS adducts, BHP hopanol-acetates, hydrogenated phytol, hydrocarbons, and wax esters were analyzed with a HP 6890 gas chromatograph (GC) equipped with a flame ionization detector (FID) and a HP-5 column (30 m × 0.25 mm, 0.25 μm film), or an HP 5890 GC equipped with a 5971 mass selective detector and a J&W Scientific DB-5ms column (60 m × 0.25 mm, 0.25 μm film). Chromatographic conditions for FAMEs were 50–120°C at 10°C min^{-1}, then at 4°C min^{-1} to 320°C, held isothermal for 3 min. Conditions for DMDS adducts were 50–120°C at 10°C min^{-1}, then at 4°C min^{-1} to 300°C, held isothermal for 30 min, then at 5°C min^{-1} to 320°C. Conditions for BHP hopanol-acetates were 90–200°C at 10°C min^{-1}, then at 4°C min^{-1} to 320°C, held isothermal for 50 min, then at 4°C min^{-1} to 340°C. Conditions for hydrogenated phytol were 50–150°C at 10°C min^{-1}, then at 4°C min^{-1} to 300°C, held isothermal for 10 min, then at 5°C min^{-1} to 320°C, held isothermal for 5 min. Conditions for hydrocarbons were 50–150°C at 5°C min^{-1}, then at 1°C min^{-1} to 240°C, then at 4°C min^{-1} to 320°C, held isothermal for 20 min. Conditions for wax esters were 50–300°C at 10°C min^{-1}, held isothermal for 60 min, then at 4°C min^{-1} to 320°C, held isothermal for 15 min.

The FAMEs were quantified on the GC-FID by using methyl tricosanoate (Sigma) as an internal standard. The BHP hopanol-acetates were quantified on the gas chromatograph–mass spectrometer (GC-MS) by using cholestanol (Sigma) as an internal standard. The hydrogenated phytols and hydrocarbons were quantified on the GC-MS by using cholestane (Sigma) and methyl tridecane (Sigma) as internal standards, respectively. The wax esters were quantified on the GC-FID by using cholestane (Sigma) as an internal standard. All quantified compounds were reported as micrograms per gram TOC.

2.6. Lipid nomenclature

Fatty acids were named according to the delta convention *X:YΔZ*, where *X* is the number of carbon atoms in the chain, *Y* is the number of unsaturations, and *Z* is the position of the unsaturation relative to the carboxyl carbon. Methyl branching at C-2 and C-3 is designated relative to the methyl end as *iso* (*i*) and *anteiso* (*a*), respectively, while midchain branching is specified relative to the carboxyl end (*e.g.,* 10-Me). Straight-chain compounds that lack branches are designated normal (*n*). Cyclopropyl compounds are indicated by the prefix *cy*.

3. Results

3.1. Chocolate Pots phototrophic mats

3.1.1. Ester-linked membrane fatty acids. The ester-linked membrane fatty acids of the phototrophic mats at Chocolate Pots were dominated by glycolipids (Table 3). The *Synechococcus*-Chloroflexi mat and the narrow *Oscillatoria* mat contained between 85% and 96% neutral and polar glycolipids, and between 4% and 15% phospholipids. The profile of the fatty acid chains in the glycolipid and phospholipid fractions of the *Synechococcus*-Chloroflexi mat revealed that the *n*-$C_{16:1}$, *n*-C_{16}, *n*-$C_{18:1}$, and *n*-C_{18} comprised approximately 83% of the fatty acids recovered (Fig. 4). Fatty acids with two double bonds (dienoic fatty acids, *n*-$C_{18:2}$) were also present in all three fractions but were highest in the neutral glycolipids ($\sim$10%). The remaining fatty acids were comprised of terminally and midchain branched compounds (0.2–8%).

For the *Synechococcus*-Chloroflexi mat, the neutral glycolipid *n*-$C_{18:1}$ contained 97% of the double bonds at the Δ9

Table 3. Basic Quantification of Different Lipid Classes Recovered from Phototrophic Mats, Ferrihydrite beneath Mats, and Ferrihydrite Adjacent to Mats at Chocolate Pots Hot Springs

Lipid class	Syn-*Cf mat core (a)*	*Ferrihydrite beneath mat (b)*	*Adjacent ferrihydrite core*	Pseudanabaena *mat*	O. princeps *mat*	*Narrow* Oscillatoria *mat channel*	*Narrow* Oscillatoria *mat terrace*
Total FAME	138,736.9	3,330.5	2,890.5	nd	nd	34,988.2	1,317.0
Phospholipids	20,564.0	391.1	323.7	nd	nd	1,250.3	68.5
Polar glycolipids	993.5	94.5	19.7	nd	nd	4,100.1	510.0
Neutral glycolipids	117,179.4	2,844.9	2,547.1	nd	nd	29,637.8	194.3
Wax esters	2,984.5	100.1	74.9	46.0	-	-	-
n-C_{17}	123.7	56.7	23.1	3,071.9	1,559.1	726.0	663.1
MMA	300.0	195.7	27.0	6,383.1	641.2	1,695.8	298.4
DMA	53.6	34.3	6.0	-	-	-	-
n-$C_{31:3}$	14.3	8.0	2.9	-	-	-	-
Hopanepolyol products	1.9	0.01	0.08	1,001.4	-	0.03	124.4

See Methods text for lipid nomenclature. Units are μg/g TOC.

Syn-Cf, *Synechococcus*-Chloroflexi mat; *O. princeps*, *Oscillatoria princeps;* FAME, fatty acid methyl esters; nd, not determined; -, not detected; MMA, monomethylalkanes; DMA, dimethylalkanes.

position, with only 3% at the Δ11 position. The polar glycolipid contained 89% of the double bonds in the Δ9 position, with 10% at Δ11 and 1% at Δ13.

3.1.2. Wax esters. Wax esters are formed by the combination of a long-chain fatty acid with a long-chain alcohol. The alcohol portion may be formed from the reduction of a fatty acid or by oxidation of a hydrocarbon (Ratledge and Wilkinson, 1988). Straight-chain saturated normal, normal (*n,n*-) wax esters dominated the wax ester profile of the *Synechococcus*-Chloroflexi mat (Table 4). The *n,n*-C_{34} and *n,n*-C_{32} were most abundant, with slightly greater quantities of the C_{34}. Wax esters with one and two *iso*-methyl moieties as *iso*, *normal*- (*i,n*-) and *iso*, *iso*- (*i,i*-), respectively, were also detected. The *Pseudanabaena* mat displayed a similar profile, except that in this mat, the *n,n*-C_{32} wax ester was more abundant than the C_{34}. Wax esters were not detected in the lower-temperature *Oscillatoria princeps* or in the narrow *Oscillatoria* mats.

3.1.3. Alkanes. The hydrocarbon fraction of the *Synechococcus*-Chloroflexi mat was dominated by normal straight-chain alkanes (*n*-C_{15} to *n*-C_{19}) (Table 4). A long-chain tri-unsaturated alkene, *n*-$C_{31:3}$, was detected. Two series of short-chain monomethylalkanes (MMAs) and one dimethylalkane (DMA) (7,11-dimethylheptadecane) were also detected and identified based on their retention times relative to the *n*-alkanes and their mass fragmentation patterns (Table 4, Fig. 5). The *Pseudanabaena*, *O. princeps*, and narrow *Oscillatoria* mats contained short-chain normal alkanes (C_{15} to C_{19}), but lacked the *n*-$C_{31:3}$ alkene (Table 4). These mats also contained the two series of MMAs but lacked any DMA (Table 4).

3.1.4. Bacteriohopanepolyols. The greatest structural variety of hopanol products was recovered by the oxidation-reduction procedure from the *Synechococcus*-Chloroflexi mat (Table 4). A homohopanol (C_{31}) and bishomohopanol (C_{32}) were detected, as well as small amounts of their 2-methyl homologues (2-MeC_{31} and 2-MeC_{32}). The homohopanol and bishomohopanol were also found in the *Pseudanabaena* and narrow *Oscillatoria* mats (Table 4). The narrow *Oscillatoria* mat in the terracette structure on the face of the main iron deposit also contained the 2-MeC_{31} BHP product.

3.2. Ferrihydrite core

The next phase of our study aimed to characterize the preservation of lipids by iron oxides. The random powder XRD patterns of the ferrihydrite beneath the *Synechococcus*-Chloroflexi mat, and the adjacent core with no conspicuous mat on the surface, revealed the presence of 2-line and 6-line ferrihydrite (Fig. 6). The two broad amorphous peaks of 2-line ferrihydrite were visible at 2.6 and 1.5 Å. Also present was the 2.2 Å peak of the slightly more ordered 6-line ferrihydrite. The broad amorphous peak of the silica phase opal-A located at $\sim$4 Å was not present.

The ester-linked fatty acids in the ferrihydrite core beneath the *Synechococcus*-Chloroflexi mat were remarkably similar to the mat but were 97.6% lower in absolute abundance (Table 3). This indicates that a reasonably high proportion of the fatty acids were remineralized to CO_2 over the scale of $\sim$2 cm. Examination of the TOC revealed a similar trend. The mat contained 1.3 wt % TOC, whereas the ferrihydrite core contained 0.2 wt % TOC (Table 2), which represents an 85% loss of TOC over the scale of $\sim$2 cm.

There did not appear to be preferential preservation of glycolipids compared to phospholipids in the ferrihydrite cores (Table 3). Both classes of fatty acids experienced 97.6–98.4% destruction. This lack of preferential preservation has also been documented in other environmental studies (Lipp *et al.,* 2008, and references therein).

Of the specific fatty acids that did escape degradation, the phospholipid, polar and neutral glycolipid profiles were again dominated by *n*-C_{16} and *n*-C_{18} fatty acids, reflecting the same distribution as was observed in the overlying mat (Fig. 4). The proportion of the dienoic fatty acid *n*-$C_{18:2}$ was highest in the neutral glycolipid fraction (10 %), as in the surface mat. The *n*-$C_{18:1}$ contained 94% of the double bond at the Δ9 position, a slight decrease from that observed in the mat, and 5% and 1% at Δ11 and Δ13, respectively.

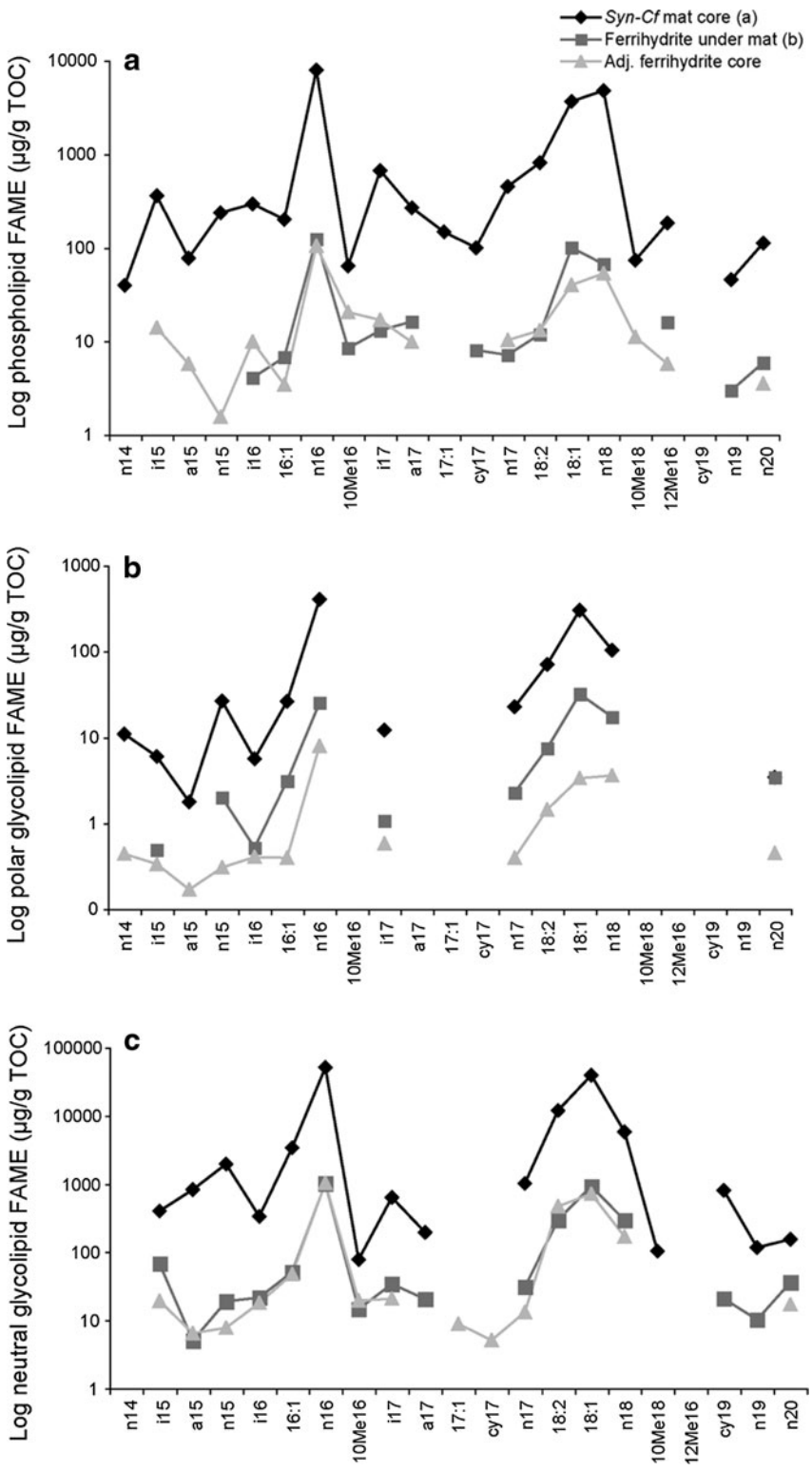

FIG. 4. (**a**) Phospholipid, (**b**) polar glycolipid, and (**c**) neutral glycolipid FAME profiles of *Synechococcus*-Chloroflexi mat, ferrihydrite core beneath mat, and adjacent ferrihydrite core lacking a conspicuous mat on the surface. Graphs were plotted on a log scale to be able to compare the subtleties of the trends.

There was a slight 2.8% increase in the *iso-, anteiso-,* and midchain branched fatty acids in the ferrihydrite core (Fig. 4). This indicates that proportionally there were slightly more chemotrophs present in the ferrihydrite than in the mat. This is not unexpected, as the lipid signature of the decomposer communities can sometimes overtake that of the primary producers (Harvey *et al.,* 1986, and references therein). However, the high percentage of n-$C_{18:1\Delta9}$ and the presence of n-$C_{18:2}$ indicate that the signature of the cyanobacteria was strongly preserved in the ferrihydrite.

The adjacent ferrihydrite sinter core with no conspicuous mat on the surface also retained a phototrophic fatty acid signature (Fig. 4), most likely inherited from mats that had colonized the surface of the sinter prior to having been entombed during mineralization. The absolute concentrations of the fatty acids were similar to those found in the

Table 4. Diagnostic Lipid Biomarkers Found in Phototrophic Mats, Ferrihydrite beneath Mats, and Ferrihydrite Adjacent to Mats at Chocolate Pots Hot Springs

Lipid biomarker	Syn-*Cf mat core (a)*	*Ferrihydrite beneath mat (b)*	*Adjacent ferrihydrite core*	Pseudanabaena *mat*	O. princeps *mat*	*Narrow* Oscillatoria *mat channel*	*Narrow* Oscillatoria *mat terrace*
Hydrocarbons							
n-C_{15}	10.8	11.5	1.1	7.8	18.3	43.2	55.9
n-C_{16}	29.9	34.3	6.5	70.3	77.6	192.1	90.8
6Me-C_{16}	33.2	39.6	3.1	128.5	107.3	328.8	52.5
5Me-C_{16}	10.2	12.2	-	28.7	0.2	66.2	-
4Me-C_{16}	12.9	14.9	1.4	25.3	34.2	136.1	-
3Me-C_{16}	-	-	1.9	58.0	42.6	165.8	-
2Me-C_{16}	12.9	15.4	1.6	51.5	34.6	112.5	-
n-$C_{17:1}$	-	-	-	-	-	141.7	49.9
n-C_{17}	123.7	56.7	23.1	3071.9	1559.1	726.0	663.1
Pristane	3.2	40.8	0.6	60.0	1.3	520.6	14.0
7Me-C_{17}	137.6	44.0	8.4	-	224.9	236.9	121.4
6Me-C_{17}	18.3	0.6	3.0	2783.6	5.3	1.8	3.3
5Me-C_{17}	16.9	21.7	2.7	2570.8	41.6	185.0	76.8
4Me-C_{17}	23.0	13.4	1.9	365.1	39.2	122.4	0.1
3Me-C_{17}	16.9	13.5	3.0	116.2	41.1	162.7	44.1
2Me-C_{17}	18.1	20.5	-	95.7	70.2	177.6	0.1
7,11DiMe-C_{17}	53.6	34.3	6.0	-	-	-	-
6Me-C_{18}	-	-	-	159.6	-	-	-
n-$C_{18:1}$	-	-	-	-	-	230.1	-
n-C_{18}	33.1	33.2	12.1	594.7	119.6	396.3	112.8
Phytane	21.9	26.8	3.2	258.1	107.7	389.1	85.3
n-C_{19}	18.6	18.3	3.1	197.5	45.8	181.5	99.4
n-$C_{31:3}$	14.3	8.0	2.9	-	-	-	-
Wax Esters							
n,n-C_{29}	5.0	3.6	1.4	0.4	-	-	-
i,n-C_{30}	7.3	0.5	0.6	0.3	-	-	-
n,n-C_{30}	51.0	1.9	1.5	2.0	-	-	-
i,n-C_{31}	23.0	9.4	2.6	1.3	-	-	-
n,n-C_{31}	97.2	3.4	2.8	4.7	-	-	-
i,i-C_{32}	5.6	-	0.5	0.3	-	-	-
i,n-C_{32}	114.4	4.2	3.5	3.6	-	-	-
n,n-C_{32}	799.8	22.5	14.3	13.6	-	-	-
i,i-C_{33}	14.3	-	1.3	-	-	-	-
i,n-C_{33}	73.2	2.8	3.6	1.9	-	-	-
n,n-C_{33}	322.9	10.2	11.3	7.1	-	-	-
i,i-C_{34}	7.7	-	0.0	-	-	-	-
i,n-C_{34}	138.8	5.0	4.5	3.0	-	-	-
n,n-C_{34}	965.9	26.9	19.4	7.4	-	-	-
i,i-C_{35}	24.3	-	0.0	-	-	-	-
i,n-C_{35}	31.0	-	1.1	-	-	-	-
n,n-C_{35}	148.9	4.0	3.7	0.2	-	-	-
i,n-C_{36}	20.9	-	0.0	-	-	-	-
n,n-C_{36}	89.9	4.1	2.4	-	-	-	-
n,n-C_{37}	43.4	1.5	0.5	-	-	-	-
Phytol	67.6	136.1	16.4	168.7	60.8	146.9	1.2
Hopanepolyol products							
2-MeC_{31}	0.02	-	-	-	-	-	10.90
C_{31}	0.21	0.01	-	26.50	-	-	7.98
2-MeC_{32}	0.02	-	-	-	-	-	-
C_{32}	1.68	0.01	0.08	974.91	-	0.03	105.51

See Methods text for lipid nomenclature. Units are μg/g TOC.
Syn-Cf, *Synechococcus*-Chloroflexi mat; *O. princeps*, *Oscillatoria princeps*; -, not detected.

ferrihydrite beneath the *Synechococcus*-Chloroflexi mat. This core was used as a control for the scanning voltammetric microelectrode measurements, and the oxygen profile reflected atmospheric diffusion and not photosynthetic oxygen production (Trouwborst *et al.,* unpublished data). Therefore, this core did not contain a biofilm of active phototrophs, and the phototrophic lipids detected were preserved.

The wax esters also persisted in the ferrihydrite cores. The relative compositions were similar to those of the mat

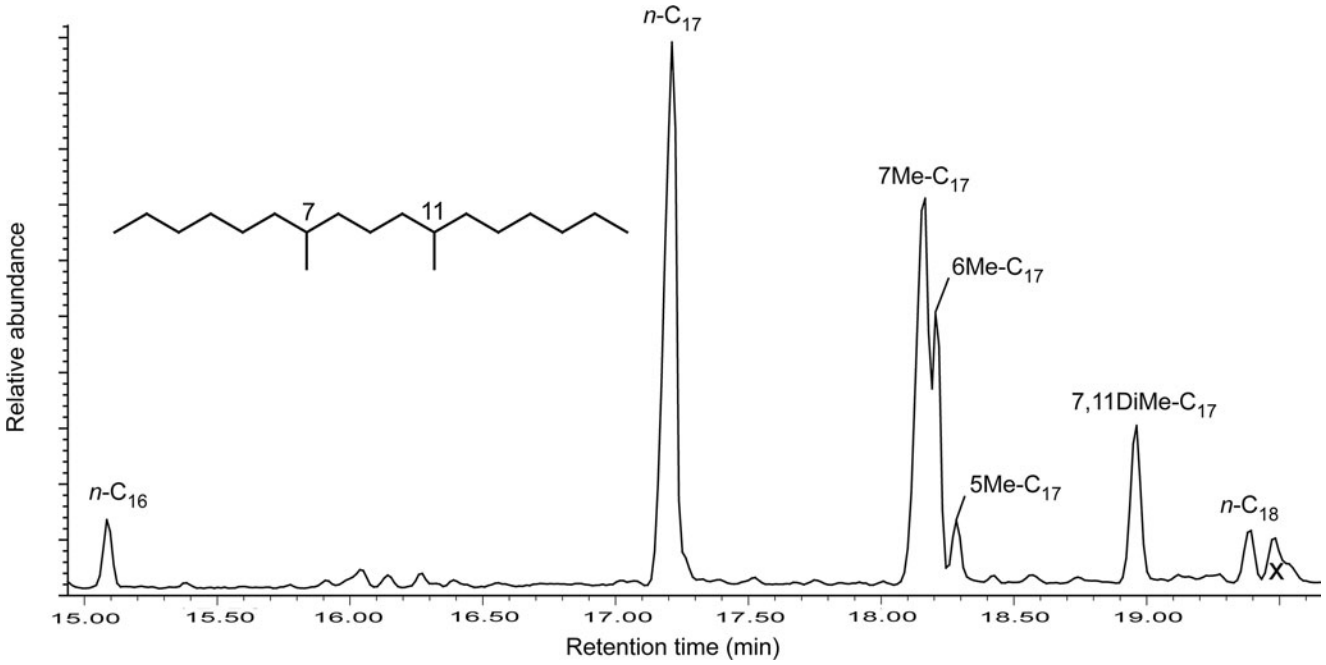

FIG. 5. Gas chromatogram of hydrocarbon fraction of *Synechococcus*-Chloroflexi mat displaying midchain branched monomethylalkanes (7-, 6-, and 5-methylheptadecanes) and one dimethylalkane (7,11-dimethylheptadecane). The x denotes a junk peak that does not correspond to a lipid.

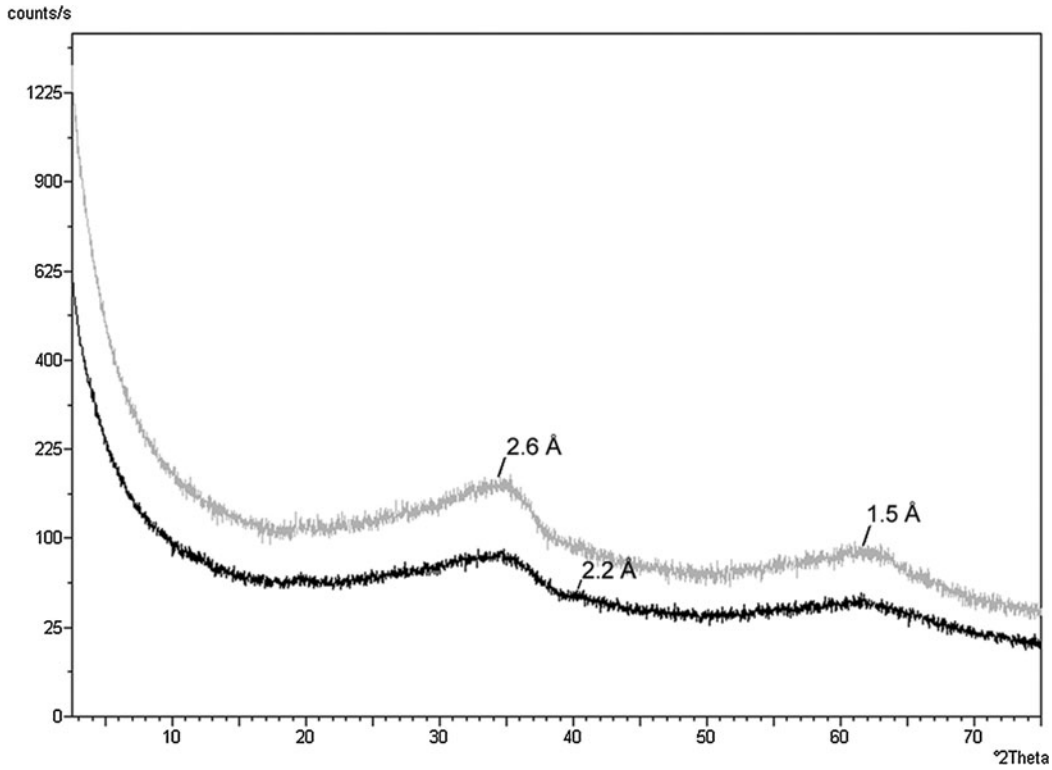

FIG. 6. Random powder XRD patterns of the iron oxide beneath the *Synechococcus*-Chloroflexi mat (gray) and the adjacent iron oxide core with no conspicuous mat on the surface (black). The two broad amorphous peaks of 2-line ferrihydrite are visible at 2.6 and 1.5 Å. Also visible in the lower pattern is the 2.2 Å peak of the slightly more ordered 6-line ferrihydrite.

with the exception of the *iso-, iso*-branched compounds, which were in the lowest abundance in the mat and not detected in the core (Table 4).

The geologically relevant alkanes detected in the *Synechococcus*-Chloroflexi mat were also present in the ferrihydrite sinter (Table 4). Most notably, the mono- and dimethylalkanes and the $C_{31:3}$ alkene survived lithification by ferrihydrite in both cores and displayed the greatest percent recovery (*i.e.,* suffered the least amount of degradation) compared to other lipid classes (Fig. 7).

The other class of geologically relevant lipids, BHPs, not surprisingly, also survived in the ferrihydrite core (Table 4). The C_{32} hopanol was the most abundant BHP product in the mats and sinter. The 2-methyl homologue (which was produced in the mat) was not detected in the ferrihydrite, probably due to its low relative abundance in the surface mat and the small sample size available for extraction. Compared to the alkanes, the BHPs displayed a relatively low percent recovery (Fig. 7).

3.3. Immature kerogen of permineralized cyanobacterial microfossils in the extinct iron-silica spring

The age of the extinct hydrothermal deposit is unknown, but a soil horizon and vegetation have developed on top of the outcrop (Fig. 3a, 3b). We are currently attempting to determine the age of the organics preserved within the deposit via C-14 dating, as has been performed for other hydrothermal sinter deposits (Lutz *et al.,* 2002). XRD of the upper band of silica in the hand sample (Fig. 3b, 3c) indicates that it is opal-A and has not yet recrystallized to quartz (Fig. 8).

The petrographic thin sections of the fossilized streamer biofabric revealed abundant amber-colored filamentous microfossils (Fig. 3d, 3e). Some microfossils were clearly identifiable as cyanobacteria, such as the well-preserved *Calothrix* filament in Fig. 3d. When viewed under ultraviolet light, the amber-colored kerogen in the microfossils fluoresced (Fig. 3f).

4. Discussion

Lipid analysis is a tool used to characterize the structure and function of extant and extinct natural microbial communities. Modern lipid studies are complementary to 16S ribosomal RNA gene analysis, -omics approaches, microscopy, pigment assays, and selective enrichments. Membrane lipids can be used to assess microbial diversity and, while arguably not as sensitive as 16S rRNA, do offer advantages in terms of characterizing how microbes respond to environmental changes (Vestal and White, 1989; Boyd *et al.,* 2011; Kaur *et al.,* 2011). Because intact polar membrane lipids (IPLs) are rapidly degraded upon cell death, they can be used to quantify live microbial biomass (White *et al.,* 1979; Lipp *et al.,* 2008). For studies that extend to the geological record, lipid classes that contain highly branched and polycyclic compounds result in fossil hydrocarbons that can survive for billions of years (Brocks *et al.,* 2003b; Brocks and Summons, 2004; Marshall *et al.,* 2007; Ventura *et al.,* 2008).

4.1. Chocolate Pots phototrophic mats

4.1.1. Ester-linked membrane fatty acids. All bacteria contain a certain amount of phospholipid in their membranes, and these ester-linked fatty acids have historically been used to assess microbial diversity (*e.g.,* White *et al.,* 1993). The fatty acid chain length, number and position of double bonds, cyclopropane rings, and position of methyl branches allow for distinction between aerobes, anaerobes, sulfate-reducing bacteria, cyanobacteria, actinomycetes, fungi, protozoa, plants, and green algae (Vestal and White, 1989, and references therein).

However, the membrane lipids of cyanobacteria and FAPs (*e.g.*, *Chloroflexus*) are primarily glycolipids, and if

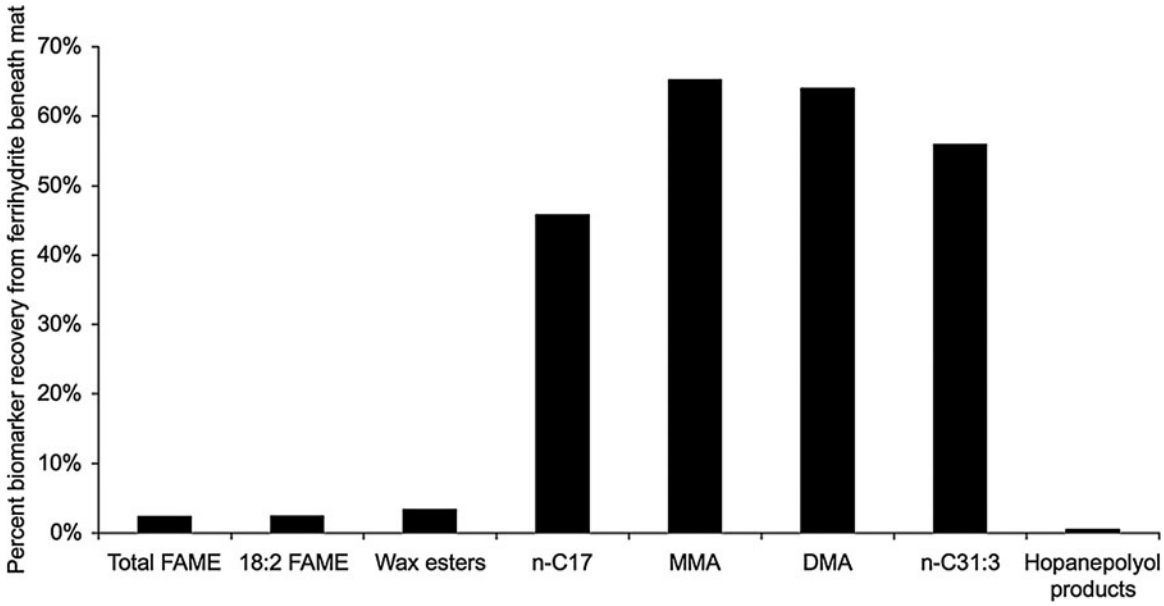

FIG. 7. Fraction of lipid biomarkers surviving in the iron oxide (ferrihydrite) beneath the phototrophic mats, expressed as percent recovery.

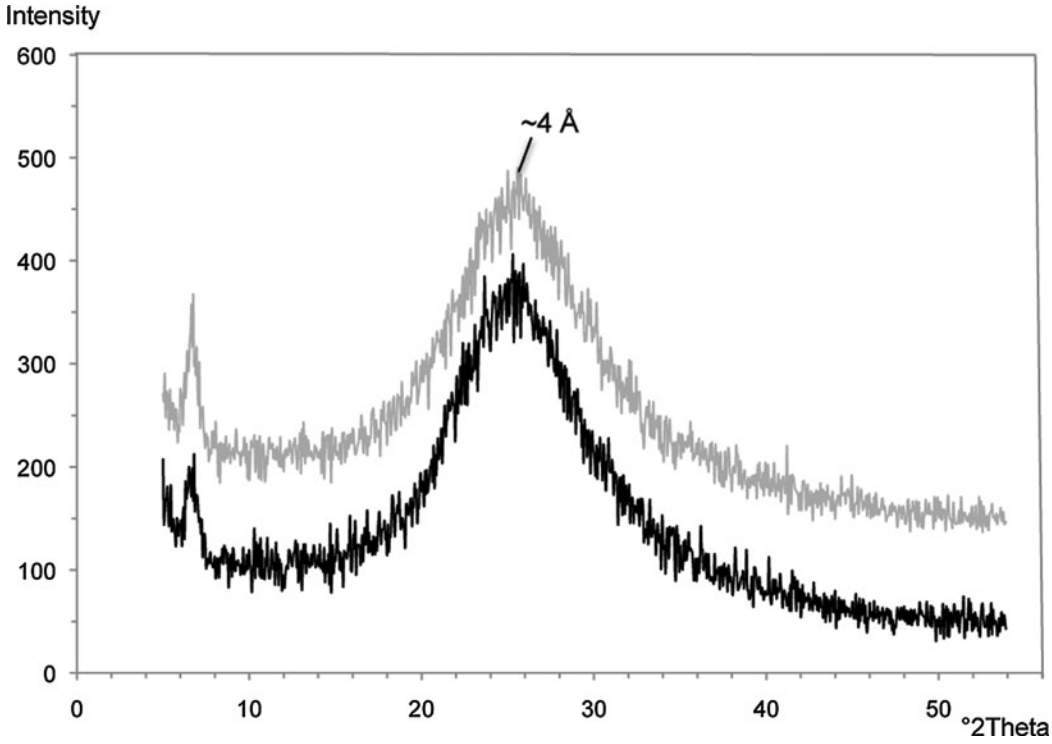

FIG. 8. Random powder XRD patterns of the mineralized biofabric from the extinct iron-silica spring shown in Fig. 3c. The opaline silica band marked by the X is shown in gray, while the siliceous iron band marked by the other X is shown in black. The broad amorphous peak of opal-A is visible at $\sim$4 Å.

only phospholipids are analyzed in natural phototrophic microbial mat samples, much taxonomic information is overlooked. Cyanobacteria predominantly contain monogalactosyl diacylglycerol (MG), digalactosyl diglyceride (DG), and sulfoquinovosyl diacylglycerol (SQ); only one phospholipid, PG, is present (*e.g.,* Fork *et al.,* 1979; Jürgens and Weckesser, 1986; Miller *et al.,* 1988; Ward *et al.,* 1994). *Chloroflexus* also contains MG, DG, and PG (Kenyon and Gray, 1974; Knudsen *et al.,* 1982, Ward *et al.,* 1994). Our methods were designed to separate the IPLs by their polar head groups into phospholipids (PG), polar glycolipids (DG), and neutral glycolipids (primarily MG and some DG) by preparative TLC (before cleavage and analysis by GC-MS). Separation by polar head groups, coupled with analysis of the acyl chain attributes, allowed for a more detailed assessment of chemotrophic versus phototrophic community members.

In terms of diagnostic fatty acid chain attributes, it should be noted that most bacterial membranes are dominated by the n-C_{16} and n-C_{18} saturated fatty acids (Ratledge and Wilkinson, 1988), which do not yield much taxonomic information. Accordingly, the n-C_{16} and n-C_{18} also dominate the fatty acid profiles of cyanobacteria and *Chloroflexus* isolates (Kenyon and Gray, 1974; Fork *et al.,* 1979; Knudsen *et al.,* 1982; Ward *et al.,* 1989). However, a more specific fatty acid biomarker for cyanobacteria is the dienoic fatty acid n-$C_{18:2}$. Dienoic fatty acids are often found in cyanobacteria (Kenyon, 1972; Kenyon *et al.,* 1972) and are produced by few other prokaryotes, particularly in hot spring environments.

Another fatty acid biomarker that can be considered of cyanobacterial origin is the n-$C_{18:1}$ with the double bond at the C-9 (Δ9) position, particularly when it is associated with the glycolipid fraction (Sakamoto *et al.,* 1994). *Chloroflexus* also synthesizes the Δ9 positional isomer (Kenyon and Gray, 1974), which we confirmed by analyzing the type strain *Chloroflexus aurantiacus* J-10-fl. The determination of double-bond position of the monounsaturated fatty acids aids in the assessment of the relative proportion of cyanobacteria and *Chloroflexus* sp. to other bacteria in these relatively simple microbial mats due to differences in the biosynthetic pathway that generates the desaturation of the acyl chain. Cyanobacteria contain an oxygen-dependent desaturation mechanism (Bloch, 1971), while other bacteria contain an anaerobic chain-elongation, dehydration system (Cronan and Rock, 1996). These different biosynthetic mechanisms result in n-$C_{18:1\Delta9}$ in cyanobacteria and n-$C_{18:1\Delta11}$ in most other bacteria. So based on the DMDS adducts of the intact fatty acids, cyanobacteria and *Chloroflexus* sp. were confirmed as the major members (89–97%) of the higher-temperature microbial mats.

Examination of the position of methyl branches on the acyl chain, particularly when the fatty acids are phospholipids, yields information about the chemotrophic community members. The detection of low levels of branched fatty acids suggests the presence of additional bacteria that were not identified in previous studies of the Chocolate Pots phototrophic mats (Fig. 5). Terminally branched *iso*- and *anteiso*-fatty acids are common in Gram-positive bacteria and sulfate-reducing bacteria. Midchain branched phospholipid fatty acids such as 10-methylhexadecanoate are considered indicative of *Desulfobacter* spp. and actinomycetes (Boschker and Middelburg, 2002). However, numerous sulfide and scanning voltammetric microelectrode

measurements of these mats in the light and the dark revealed no detectable sulfide (Pierson *et al.,* 1999; Trouwborst *et al.,* 2007). Additionally, no sulfur-containing minerals were detected by XRD or energy-dispersive spectroscopy (Parenteau and Cady, 2010), further suggesting the absence of a detectable sulfur cycle. This was supported by the lack of sulfate-reducing bacteria in the metagenomic data of the Chocolate Pots mat (Klatt *et al.,* 2013). Therefore, actinomycetes are the most probable source of the 10-methyl fatty acids and were likely derived from the soil immediately adjacent to the hot springs. Thermophilic chemolithotrophic iron oxidizers are probably not present in this system; microscopic examination of surface samples taken at the vent, and at 1 m intervals away from the vent, did not reveal obvious morphological evidence of iron oxidizers (Emerson and Weiss, 2004). Attempts at isolating the organisms with gradient and liquid enrichment techniques were also unsuccessful (Emerson and Weiss, 2004).

In terms of other sources of methyl-branched fatty acids, it has been shown that certain species of cyanobacteria from Antarctica synthesize terminally branched *iso*- and *anteiso*-fatty acids (Rezanka *et al.,* 2009), which may explain our detection of these compounds given the lack of sulfate-reducing bacteria in this system. To date, it has been shown that *Chloroflexus auranticus* does not synthesize these branched fatty acids (Knudsen *et al.,* 1982). However, the presence of numerous branched wax esters in *Chloroflexus*-containing mats throughout the thermal features of Yellowstone (*e.g.,* van der Meer *et al.,* 2003; Jahnke *et al.,* 2004) strongly suggests that some species of *Chloroflexus* do synthesize branched fatty acids, which are necessary biosynthetic precursors to these compounds.

4.1.2. Wax esters. Wax esters are considered biomarkers for the FAPs *Chloroflexus* and *Roseiflexus* (Knudsen *et al.,* 1982; Shiea *et al.,* 1991; van der Meer *et al.,* 1999, 2002). The wax esters and $C_{31:3}$ alkene (discussed below in the alkane section) support the presence of *Chloroflexus* in the *Synechococcus* mat at Chocolate Pots. What is surprising is the lack of the $C_{31:3}$ and abundance of wax esters in the *Pseudanabaena* mat, which suggests the presence of *Roseiflexus* sp. *Roseiflexus* is probably also likely present in the *Synechococcus* mat, despite the lack of a characteristic red layer beneath the upper green cyanobacterial layer. This is the first detection of *Roseiflexus* spp. in a slightly acidic iron-rich hot spring, as they are typically found in alkaline silica-depositing hot springs (Boomer *et al.,* 2000; Hanada and Pierson, 2002; Nübel *et al.,* 2002; Madigan *et al.,* 2005; van der Meer *et al.,* 2005; Klatt *et al.,* 2007).

4.1.3. Alkanes. Normal straight-chain alkanes are the most abundant hydrocarbons in all nonbiodegraded oils and mature bitumens in the rock record (Brocks and Summons, 2004). Many eukaryotes and a few prokaryotes synthesize alkanes, which are derived from fatty acids via an enzymatic decarboxylation mechanism (Albro, 1976; Schirmer *et al.,* 2010). In addition to direct enzymatic production, alkanes can be derived from the diagenesis of other biological precursor lipids and from the catagenesis of kerogens (*e.g.,* Boschker and Middelburg, 2002).

Midchain methyl-branched alkanes, such as the monomethylhexa- and heptadecanes and 7,11-dimethylheptadecane identified here, are considered biomarkers for cyanobacteria (Han and Calvin, 1969; Shiea *et al.,* 1990, 1991; Kenig *et al.,* 1995; Jahnke *et al.,* 2004). MMAs have been documented in a large number of pure cultures of cyanobacteria and in natural cyanobacterial mats (Shiea *et al.,* 1990, and references therein; Zeng *et al.,* 1992; Kenig *et al.,* 1995; Dembitsky *et al.,* 2001; Jahnke *et al.,* 2004). DMAs have been found in cyanobacterial mats throughout the world (Robinson and Eglinton, 1990; Shiea *et al.,* 1990; Kenig *et al.,* 1995; Jahnke *et al.,* 2004), but they have been characterized in only a few cyanobacterial cultures (Summons *et al.,* 1996; Köster *et al.,* 1999; Jahnke *et al.,* 2004). In Yellowstone, DMAs have only been reported in a *Phormidium* mat from the silica-depositing alkaline chloride springs at Fountain Paint Pots (Jahnke *et al.,* 2004). This report of 7,11-dimethylheptadecane is the first for (1) a *Synechococcus*-Chloroflexi mat and (2) a slightly acidic iron-depositing hot spring.

The $C_{31:3}$ alkene is considered a biomarker for *Chloroflexus* (van der Meer *et al.,* 1999). The detection of this alkene and the wax esters in the higher-temperature *Synechococcus*-Chloroflexi mat confirms the previous identification of *Chloroflexus* in this mat by phase and near-infrared epifluorescence microscopy and *in vivo* pigment analyses (Pierson and Parenteau, 2000).

4.1.4. Bacteriohopanepolyols. Hopanoids are considered the most abundant natural product on Earth (Ourisson and Albrecht, 1992) and are ubiquitous in sedimentary organic matter and petroleum of all geological eras (Brocks and Summons, 2004). The functionalized bacterial precursors of sedimentary hopanoids or hopanes are BHPs. BHPs are pentacyclic triterpanoids with a hopane skeleton linked to a variety of polyhydroxylated side chains (Ourisson *et al.,* 1987; Summons *et al.,* 1999). They are synthesized by a wide variety of cultured aerobic and facultative anaerobic bacteria (Rohmer *et al.,* 1984; Farrimond *et al.,* 2000) and a few strict anaerobes (Sinninghe Damsté *et al.,* 2004; Fischer *et al.,* 2005).

Modification of the hopanoid skeleton by alkyl substituents can occur at either C-2 or C-3. Methylation at C-2 is characteristic of a high proportion of cyanobacteria, particularly those isolated from hot springs, and is considered a biomarker for this group (Summons *et al.,* 1999). This finding was supported by Talbot *et al.* (2008) in an extended survey of intact BHPs in marine, freshwater, and hydrothermal cyanobacterial cultures and in environmental samples from lakes, hot and cold deserts, and hydrothermal springs. However, 2-methyl(Me)BHP has been found in one nonmarine purple nonsulfur phototroph, *Rhodopseudomonas palustris* TIE-1 (Rashby *et al.,* 2007), calling into question the utility of this compound as a biomarker for cyanobacteria. But the very low numbers of alphaproteobacterial sequences (and complete lack of purple nonsulfur sequences) retrieved from the Chocolate Pots *Synechococcus*-Chloroflexi mat metagenomic data and supporting 16S rRNA panels (Klatt *et al.,* 2013) suggest that, in this system, 2-MeBHP is a biomarker for cyanobacteria.

The same 2-MeC_{31} and 2-MeC_{32} hopanol products recovered from the Chocolate Pots mats were also found in the Yellowstone *Phormidium* mats at Fountain Paint Pots and have been identified in a New Zealand hot spring isolate,

Oscillatoria amphigranulata (Castenholz and Utkilen, 1984; Jahnke *et al.,* 2004). Interestingly, there were no methylated BHPs found in the *Synechococcus*-Chloroflexi mat at Octopus hot springs (Talbot *et al.,* 2008).

This examination of modern, functionalized lipids in the Chocolate Pots iron mats compares well to the extensive body of work performed on the phototrophic mats at the alkaline chloride silica-depositing Octopus Spring in Yellowstone (*e.g.,* Ward *et al.,* 1989, 1994; Shiea *et al.,* 1990, 1991; Zeng *et al.,* 1992; Summons *et al.,* 1996; van der Meer *et al.,* 1999, 2002, 2010). The *Synechococcus*-Chloroflexi mats from both locales are remarkably similar in terms of lipid and community-member composition, despite their vastly different geochemical environments. These observations are supported by a recent metagenomics study, which revealed that the Chocolate Pots *Synechococcus* sp. were most similar to the *Synechococcus* sp. B′-like populations observed in Octopus and Mushroom Springs, despite the differences in pH ($\sim$6 vs. $>$8) (Klatt *et al.,* 2013).

The next phase of our study aimed to characterize the preservation of lipids by iron oxides. There has been substantial work done that has examined the preservation of lipids by silica in New Zealand hot springs, although these studies focused on higher-temperature ($\sim$75°C) communities dominated by bacteria (*e.g.,* Aquificales) and archaea (*e.g.,* Sulfolobales) (Pancost *et al.,* 2005, 2006; Talbot *et al.,* 2005; Gibson *et al.,* 2008; Kaur *et al.,* 2008, 2011). The primary mode of preservation in silica-depositing springs is rapid silicification and entombment within the silica matrix. This mechanism will be contrasted with hypotheses for the iron system.

4.2. Ferrihydrite core

This portion of the study aimed to determine which lipid classes survived microbial degradative processes in the mats. Another goal was to determine how mineralization of the mats by siliceous 2-line ferrihydrite, the primary iron phase of the sinter, affected the lipid signature of the microbial community.

In general, there appears to be some degree ($\sim$15%) of bulk TOC preservation in the ferrihydrite core beneath the cyanobacterial mats at Chocolate Pots. We speculate that iron may play a role in this preservation process. Recently, a mechanism involving iron-enhanced preservation of organic carbon was described in marine sediments (Lalonde *et al.,* 2012). It was shown that iron directly chelates or coprecipitates with the organic carbon, generating a ''rusty sink'' which functions in the long-term storage of organics. This is in contrast to the prevailing view that iron oxidizes organics and thus destroys them (Klein, 2005).

In addition to the bulk TOC preservation, we unexpectedly recovered labile cyanobacterial and *Chloroflexus* phospholipids and glycolipids from the ferrihydrite core. These IPLs are rapidly degraded after cell death by the cell's own lytic enzymes or those of decomposers (Harwood and Russell, 1984). As a result, they are used as indicators of cellular viability in natural environments (White *et al.,* 1997; Lipp *et al.,* 2008). We did not anticipate finding any phototrophic IPLs buried in the ferrihydrite core. A possible explanation is that it has been shown that iron may inhibit cellular autolytic enzymes (Herbold and Glaser, 1975; Leduc *et al.,* 1982). Inhibition of the cell's own lytic enzymes, or those of heterotrophs, may promote the survival of lipids during cell death and heterotrophic grazing and thus increase the yield of lipids potentially entering the rock record.

Another possible explanation for the IPL recovery is that our previous microscopic study of microfossil formation in this system revealed that the photosynthetic membrane structures in the cyanobacterial cells were well preserved via ferrihydrite permineralization (Parenteau and Cady, 2010). The ferrihydrite appeared to be physically binding to the membranes, which may make the IPLs unavailable to enzymatic attack.

The geologically relevant phototrophic lipid biomarkers were also preserved in the ferrihydrite core beneath the cyanobacterial mats. Both normal and branched alkanes displayed the greatest percent recovery or least amount of degradation (Fig. 7). Alkanes have proven to be relatively recalcitrant hydrocarbon biomarkers and have been characterized from many ancient sediments, such as Holocene cyanobacterial mats (Kenig *et al.,* 1995) and the 2.78–2.45 Ga shales of the Mount Bruce Supergroup in the Pilbara Craton (Brocks *et al.,* 2003a, 2003b).

Compared to the alkanes, the BHPs displayed a lower percent recovery (Fig. 7). We hypothesize that this may be due to the chemical binding of the polyhydroxylated side chain by iron, which may require more severe chemical treatment to recover. The iron-chelating/coprecipitation mechanism described by Lalonde *et al.* (2012) may also be functioning in the binding of the BHPs. It has been previously shown that reaction of sulfur with unsaturated and polyfunctional organic compounds (sulfurization) enhances preservation by promoting the incorporation of these compounds into the macromolecular structure of kerogen (Sinninghe Damsté *et al.,* 1989; Sinninghe Damsté and de Leeuw, 1990; Kohnen *et al.,* 1991). We hypothesize that a similar scenario could be happening with the lipid functional groups and the ferrihydrite, and that use of a more destructive method could increase hopanoid recovery.

4.3. Immature kerogen of permineralized cyanobacterial microfossils

The purpose of this portion of the project was to assess organic matter preservation in an extinct iron-silica spring located $\sim$700 m north of Chocolate Pots. These deposits have undergone later stages of diagenesis. The earliest diagenetic window in the extant microbial mats in the active hot spring encompassed lipid biomarker production and survival through microbial degradation and mineral binding and encrustation onto biological surfaces, and mineral infusion of porous organic materials (*i.e.,* permineralization). We hypothesized that the extinct hydrothermal deposits would allow us to assess the fate of organics upon recrystallization of the primary precipitates to more ordered phases, pore-filling of the mineral matrix, and reaction with later stage redox-reactive fluids.

We anticipated that the silica and iron bands in the extinct sinter would reflect later diagenetic phases such as quartz, goethite, or hematite. However, XRD of the upper band of silica in the hand sample (Fig. 3b, 3c) indicated that the amorphous opal-A has not yet recrystallized to more stable phases like cristobalite, tridymite, or quartz. However, the

persistence of opal-A does not necessarily indicate that the deposit is exceptionally young. The oldest known siliceous sinters in Yellowstone are located at Artist Point and are thought to have formed between 600 and 130 ka (White *et al.,* 1988). The silica phases identified in the Artist Point sinters include opal-A, opal-CT, and quartz (Hinman and Walter, 2005). The detection of opal-A in the Artist Point sinters indicates that recrystallization can take several hundred thousand years. So the extinct iron-silica sinter near Chocolate Pots may be as old as the Artist Point sinters, as it does display significant postdepositional cementation.

The organics in the cyanobacterial microfossils in the extinct sinter appeared to be well preserved. Given the high transmissivity and intense fluorescence of the kerogen macerals, it is likely immature liptinite. Other maceral groups such as vitrinite and inertinite do not fluoresce. Liptinite is composed of degraded lipids and other low-molecular-weight compounds that have been incorporated into complex geopolymers by condensation and defunctionalization reactions (Stasiuk, 1994). These geopolymers, along with selectively preserved biopolymers that are resistant to microbial degradation (such as hopanoids) (Tegelaar *et al.,* 1989) and highly aliphatic macromolecules in the cell walls of cyanobacteria (Chalansonnet *et al.,* 1988), are likely important contributors to the immature kerogen in the microfossils and the finely dispersed kerogen in the streamer biofabric. In future studies we will use time-of-flight secondary mass spectroscopy to nondestructively characterize the lipids in the microfossils (*e.g.*, Siljeström *et al.,* 2010).

4.4. Early diagenesis in modern iron-silica springs

This study attempted to characterize the fate of organic material through two diagenetic windows in an iron-silica hydrothermal system: one in the extant microbial mats and the other in subrecent sinter deposits. The first taphonomic window included the production and survival of labile (*e.g.,* fatty acids and wax esters) and refractory, geologically relevant (*e.g.,* branched alkanes and hopanoids) lipids in the *Synechococcus*-Chloroflexi mat. It is in this window that most of the organic matter is destroyed (*i.e.,* remineralized) via microbial degradation (photoheterotrophy, aerobic respiration, anaerobic respiration, fermentation, and methanogenesis) (Brocks and Summons, 2004). These metabolic processes have been documented to occur in hot spring mats and have been well studied in the *Synechococcus*-Chloroflexi mat at Octopus and Mushroom Springs (Zeikus *et al.,* 1980; Ward *et al.,* 1998; Dillon *et al.,* 2007). Of these processes, aerobic respiration is probably the most important in organic matter degradation and is controlled by the availability of oxygen.

We expected to see nearly 100% remineralization of labile compounds. Instead, there appeared to be some degree of survival of fatty acids (97.6% loss) and TOC (85% loss). This may be due to the presence of anoxic, Fe(II)-rich waters that bathe the mats. Our scanning voltammetric microelectrode studies have shown that the oxygen produced by the cyanobacteria in the upper layers of the *Synechococcus*-Chloroflexi mat does not accumulate to supersaturated levels as it does in the *Synechococcus*-Chloroflexi mats at Octopus (Trouwborst *et al.,* 2007). The oxygen production rate is balanced by consumption by the constant influx of Fe(II) from the vent. The resulting net lower oxygen levels may depress aerobic respiration rates, thereby consuming less organic matter.

Iron may play other roles in enhancing the early preservation of lipids. As mentioned previously, the iron may inhibit the phototrophs' autolytic enzymes that hydrolyze various organic moities upon death, and may inhibit those of heterotrophs as well. Iron can also chemically bind or chelate the organic compounds. In studies of microfossil formation, it has been shown that the electrostatic interaction of the positively charged iron (and potentially other cations) with the predominantly negatively charged cell surface functional groups (*e.g.,* Ferris *et al.,* 1988; Warren and Ferris, 1998; Phoenix *et al.,* 2003) leads to rapid mineralization of the cells. This entombment by iron may make the cells less available to enzymatic attack. It may also facilitate silicification and enhance microfossil preservation by acting as a cation bridge between the negatively charged cell surface and negatively charged silicic acid (*e.g.,* Ferris *et al.,* 1988; Urrutia and Beveridge 1993, 1994; Fortin *et al.,* 1997). The ''rapid entombment'' mechanism has also been invoked to explain the preservation of lipids in silica-depositing springs in New Zealand (*e.g.,* Kaur *et al.,* 2011).

The preceding discussion identifies ways in which iron may facilitate the preservation of organic material. However, it has also been suggested that iron directly oxidizes organics it comes in contact with and effectively destroys them (Klein, 2005). Because of this, we anticipated no net entry of organic material into the ferrihydrite sinter beneath the mats, or any kerogen in the extinct iron-silica deposits. But it must be noted that primary nanophase iron oxyhydroxide precipitates (ferrihydrite) frequently coprecipitate with silica, which adsorbs to the surface to form siliceous ferrihydrite (*e.g.,* Carlson and Schwertmann, 1981; Schwertmann *et al.,* 1984; Cornell *et al.,* 1987; Parfitt *et al.,* 1992). It has been shown that this silica blocks surface unsaturated Fe-coordination sites (*e.g.,* Carlson and Schwertmann, 1981; Schwertmann *et al.,* 1984; Cornell *et al.,* 1987; Zhao *et al.,* 1994), which effectively makes them unavailable to extract electrons from organic material. This process may enhance early preservation of organics in iron-silica systems. However, it should be noted that ferrihydrite is a metastable phase that will recrystallize to more ordered forms such as hematite or goethite. The adsorbed Si is apparently released at this stage and precipitates as a separate, secondary phase (Harder, 1963). Potentially, during this later diagenetic window, organics may be destroyed as surface Fe sites are once again exposed.

4.5. Relevance to early Earth and Mars

The oldest known subaerial hydrothermal deposits on Earth are found in the Drummond Basin, Australia, and have been dated at 342–298 Ma (Walter *et al.,* 1996). The Verbena sinters contain thin-bedded microfacies with streamer biofabrics that are closely comparable to sinters in Yellowstone (Walter *et al.,* 1996). They are composed of laminae of iron-stained microcrystalline quartz (chert) and appear to be analogous to the extinct iron-silica deposit near Chocolate Pots.

We recognize that the nature of lipid biomarker and kerogen preservation observed in this study occurred early

in the diagenetic history of the Chocolate Pots sinter deposits; however, it is clear that at the earliest stage, fossil biosignatures have survived the initial stages of diagenesis. Taphonomic studies of biosignature preservation in modern microbial ecosystems that evaluate the impacts of early diagenesis can lead to an improved understanding of paragenetic histories in iron and silica hydrothermal systems and the impacts on fossil preservation.

This strategy is particularly relevant when searching for evidence of extinct microbial life in similar deposits on Mars, such as the amorphous silica deposits (opal-A) at Home Plate in Gusev Crater. These silica deposits were detected by the NASA Spirit rover and have been interpreted as evidence of a martian hydrothermal spring system (Ruff *et al.,* 2011). Because spectral analyses suggest that the opal-A has not recrystallized to quartz, it makes a case for examining the fate of organics through early diagenesis in modern and subrecent hydrothermal sinters on Earth that also have not undergone extensive recrystallization. The systematic documentation of microbial biosignatures (biofabrics, microfossils, and lipid biomarkers) in modern hydrothermal springs can lay important groundwork in the search for evidence of fossilized microbial life in analogous deposits on Mars.

Acknowledgments

This work was supported by NASA Exobiology Grant NAG5-12328. Additional support was generously provided by a NASA Oregon Space Grant Graduate Fellowship, a NASA Planetary Biology Internship, and a NASA Postdoctoral Program Fellowship to M.N. Parenteau. Part of this work was supported by grants from the NASA Exobiology Program (NNX08AZ47A) to L. Jahnke and the NASA Mars Fundamental Research Program (NNH08ZDA001N) to J.D. Farmer. S.L. Cady acknowledges financial support from the Environmental and Molecular Sciences Laboratory (EMSL), a national scientific user facility sponsored by the Department of Energy's Office of Biological and Environmental Research and located at Pacific Northwest National Laboratory, and from the NASA Exobiology Program (NNX11AR81G). We thank the National Park Service for allowing us to conduct research in Yellowstone National Park and thank Mike Kubo and Tsegereda Embaye, SETI Institute; Kendra Turk, University of California Santa Cruz; and Georg Grathoff, Portland State University for technical assistance. We thank Dave Des Marais and Beverly Pierson for helpful discussions and two anonymous reviewers, who helped strengthen the manuscript.

Author Disclosure Statement

No competing financial interests exist.

Abbreviations

ASC, acid-sulfate-chloride.
BHPs, bacteriohopanepolyols.
DG, digalactosyl diglyceride.
DMA, dimethylalkane.
DMDS, dimethyl disulfide.
FAMEs, fatty acid methyl esters.
FAPs, filamentous anoxygenic phototrophs.
FID, flame ionization detector.
GC, gas chromatograph.
GC-MS, gas chromatograph–mass spectrometer.
IPLs, intact polar membrane lipids.
MG, monogalactosyl diacylglycerol.
MMAs, monomethylalkanes.
PG, phosphatidylglycerol.
TLC, thin-layer chromatography.
TOC, total organic carbon.
XRD, X-ray diffraction.

References

Albro, P.W. (1976) Bacterial waxes. In *Chemistry and Biochemistry of Natural Waxes,* edited by P.E. Kolatukudys, Elsevier, Amsterdam, pp 419–445.

Baratoux, D., Toplis, M.J., Monnereau, M., and Gasnault, O. (2011) Thermal history of Mars inferred from orbital geochemistry of volcanic provinces. *Nature* 472:338–341.

Benning, L.G., Phoenix, V.R., Yee, N., and Tobin, M.J. (2004) Molecular characterization of cyanobacterial silicification using synchrotron infrared micro-spectroscopy. *Geochim Cosmochim Acta* 68:729–741.

Bloch, K. (1971) B-hydroxydecanoyl thioester dehydrase. In *The Enzymes,* edited by P.D. Boyers, Academic Press, New York, pp 441–464.

Boomer, S.M., Pierson, B.K., Austinhirst, R., and Castenholz, R.W. (2000) Characterization of novel bacteriochlorophyll-*a*-containing red filaments from alkaline hot springs in Yellowstone National Park. *Arch Microbiol* 174:152–161.

Boschker, H.T.S. and Middelburg, J.J. (2002) Stable isotopes and biomarkers in microbial ecology. *FEMS Microbiol Ecol* 40:85–95.

Boyd, E.S., Pearson, A., Pi, Y., Li, W.J., Zhang, Y.G., He, L., Zhang, C.L., and Geesey, G.G. (2011) Temperature and pH controls on glycerol dibiphytanyl glycerol tetraether lipid composition in the hyperthermophilic crenarchaeon *Acidilobus sulfurireducens*. *Extremophiles* 15:59–65.

Brock, T.D. (1967) Life at high temperatures. *Science* 158: 1012–1019.

Brock, T.D. (1978) *Thermophilic Microorganisms and Life at High Temperatures,* Springer-Verlag, New York.

Brocks, J.J. and Summons, R.E. (2004) Sedimentary hydrocarbons, biomarkers for early life. In *Biogeochemistry: Treatise on Geochemistry, Volume 8,* edited by W.H. Schlesinger, Elsevier Pergamon, Oxford, pp 63–115.

Brocks, J.J., Buick, R., Logan, G.A., and Summons, R.E. (2003a) Composition and syngeneity of molecular fossils from the 2.78 to 2.45 billion-year-old Mount Bruce Supergroup, Pilbara Craton, Western Australia. *Geochim Cosmochim Acta* 67:4289–4319.

Brocks, J.J., Buick, R., Summons, R.E., and Logan, G.A. (2003b) A reconstruction of Archean biological diversity based on molecular fossils from the 2.78 to 2.45 billion-year-old Mount Bruce Supergroup, Hamersley Basin, Western Australia. *Geochim Cosmochim Acta* 67:4321–4335.

Cady, S.L. and Farmer, J.D. (1996) Fossilization processes in siliceous thermal springs: trends in preservation along thermal gradients. In *Evolution of Hydrothermal Ecosystems on Earth (and Mars?),* Ciba Foundation Symposium 202, edited by G.R. Bock and J.A. Goode, John Wiley and Sons, Chichester, UK, pp 150–173.

Cady, S.L., Farmer, J.D., Grotzinger, J.P., Schopf, J.W., and Steele, A. (2003) Morphological biosignatures and the search for life on Mars. *Astrobiology* 3:351–368.

Carlson, L. and Schwertmann, U. (1981) Natural ferrihydrites in surface deposits from Finland and their association with silica. *Geochim Cosmochim Acta* 45:421–429.

Castenholz, R.W. (1969) Thermophilic blue-green algae and the thermal environment. *Bacteriol Rev* 33:476–504.

Castenholz, R.W. (1988) Culturing methods for cyanobacteria. *Methods Enzymol* 167:68–93.

Castenholz, R.W. and Utkilen, H.C. (1984) Physiology of sulfide tolerance in a thermophilic *Oscillatoria*. *Arch Microbiol* 138:299–305.

Chalansonnet, S., Largeau, C., Casadevall, E., Berkaloff, C., Peniguel, G., and Couderc, R. (1988) Cyanobacterial resistant biopolymers. Geochemical implications of the properties of *Schizothrix* sp. resistant material. *Org Geochem* 13:1003–1010.

Cornell, R.M., Giovanoli, R., and Schindler, P.W. (1987) Effect of silicate species on the transformation of ferrihydrite into goethite and hematite in alkaline media. *Clays Clay Miner* 35:12–28.

Cronan, J.E. and Rock, C.O. (1996) Biosynthesis of membrane lipids. In Escherichia coli *and* Salmonella: *Cellular and Molecular Biology,* 2nd ed., edited by F.C. Neidhardt, R. Curtiss III, J.L. Ingraham, E.C.C. Lin, K.B. Low, B. Magasanik, W.S. Reznikoff, M. Riley, M. Schaechter, and H.E.S. Umbarger, ASM Press, Washington, DC, pp 612–636.

Dembitsky, V.M., Dor, I., Shkrob, I., and Aki, M. (2001) Branched alkanes and other apolar compounds produced by the cyanobacterium *Microcoleus vaginatus* from the Negev Desert. *Russian Journal of Bioorganic Chemistry* 27: 110–119.

Dillon, J.G., Fishbain, S., Miller, S.R., Bebout, B.M., Habicht, K.S., Webb, S.M., and Stahl, D.A. (2007) High rates of sulfate reduction in a low-sulfate hot spring microbial mat are driven by a low level of diversity of sulfate-respiring microorganisms. *Appl Environ Microbiol* 73:5218–5226.

Emerson, D. and Weiss, J.V. (2004) Bacterial iron oxidation in circumneutral freshwater habitats: findings from the field and the laboratory. *Geomicrobiol J* 21:405–414.

Farmer, J.D. (1995) Mars exopaleontology. *Palaios* 10: 197–198.

Farmer, J.D. (1996) Hydrothermal processes on Mars: an assessment of present evidence. In *Evolution of Hydrothermal Ecosystems on Earth (and Mars?),* Ciba Foundation Symposium 202, edited by G.R. Bock and J.A. Goode, John Wiley and Sons, Chichester, UK, pp 273–299.

Farmer, J.D. (1999) Taphonomic modes in microbial fossilization. In *Size Limits of Very Small Microorganisms: Proceedings of a Workshop,* National Research Council, The National Academies Press, Washington, DC, pp 94–102.

Farmer, J.D. (2003) Exploring for a fossil record of extraterrestrial life. In *Paleobiology II,* edited by D.E.G. Briggs and P.R.S. Crowther, Blackwell Science, Malden, MA, pp 8–13.

Farmer, J.D. and Des Marais, D.J. (1999) Exploring for a record of ancient martian life. *J Geophys Res* 104:26977–26995.

Farrimond, P., Head, I.M., and Innes, H.E. (2000) Environmental influence on the biohopanoid composition of recent sediments. *Geochim Cosmochim Acta* 64:2985–2992.

Fernández-Remolar, D.C. and Knoll, A.H. (2008) Fossilization potential of iron-bearing minerals in acidic environments of Río Tinto, Spain: implications for Mars exploration. *Icarus* 194:72–85.

Fernández-Remolar, D.C., Morris, R.V., Gruener, J.E., Amils, R., and Knoll, A.H. (2005) The Río Tinto Basin, Spain: mineralogy, sedimentary geobiology, and implications for interpretation of outcrop rocks at Meridiani Planum, Mars. *Earth Planet Sci Lett* 240:149–167.

Ferris, F.G. and Magalhaes, E. (2008) Interfacial energetics of bacterial silicification. *Geomicrobiol J* 25:333–337.

Ferris, F.G., Fyfe, W.S., and Beveridge, T.J. (1988) Metallic ion binding by *Bacillus subtilis:* implications for the fossilization of microorganisms. *Geology* 16:149–152.

Fischer, W.W., Summons, R.E., and Pearson, A. (2005) Targeted genomic detection of biosynthetic pathways: anaerobic production of hopanoid biomarkers by a common sedimentary microbe. *Geobiology* 3:33–40.

Fork, D.C., Murata, N., and Sato, N. (1979) Effect of growth temperature on the lipid and fatty acid composition, and the dependence on temperature of light-induced redox reactions of cytochrome *f* and of light energy redistribution in the thermophilic blue-green alga *Synechococcus lividus*. *Plant Physiol* 63:524–530.

Fortin, D., Ferris, F.G., and Beveridge, T.J. (1997) Surface-mediated mineral development by bacteria. *Reviews in Mineralogy and Geochemistry* 35:161–180.

Fournier, R.O. (1989) Geochemistry and dynamics of the Yellowstone National Park hydrothermal system. *Annu Rev Earth Planet Sci* 17:13–53.

Gibson, R.A., Talbot, H.M., Kaur, G., Pancost, R.D., and Mountain, B. (2008) Bacteriohopanepolyol signatures of cyanobacterial and methanotrophic bacterial populations recorded in a geothermal vent sinter. *Org Geochem* 39:1020–1023.

Giggenbach, W.F. (1988) Geothermal solute equilibria. Derivation of Na-K-Mg-Ca geoindicators. *Geochim Cosmochim Acta* 52:2749–2765.

Han, J. and Calvin, M. (1969) Hydrocarbon distribution of algae and bacteria, and microbiological activity in sediments. *Proc Natl Acad Sci USA* 64:436–443.

Hanada, S. and Pierson, B.K. (2002) The family Chloroflexaceae. In *The Prokaryotes: An Evolving Electronic Resource for the Microbiological Community,* 3rd ed., Release 3.11, November 22, 2002, edited by M.E.A. Dworkins, Springer-Verlag, New York.

Harder, H. (1963) Zur diskussion uber die entstehung der quarzbandererze (itabirite). *Neues Jahrbuch fur Mineralogie-Monatshefte* 12:303–314.

Harvey, H.R., Fallon, R.D., and Patton, J.S. (1986) The effect of organic matter and oxygen on the degradation of bacterial membrane lipids in marine sediments. *Geochim Cosmochim Acta* 50:795–804.

Harwood, J.L. and Russell, N.J. (1984) *Lipids in Plants and Microbes,* George Allen and Unwin, London.

Herbold, D.R. and Glaser, L. (1975) *Bacillus subtilis N*-acetylmuramic acid L-alanine amidase. *J Biol Chem* 250:1676–1682.

Hinman, N.W. and Walter, M.R. (2005) Textural preservation in siliceous hot spring deposits during early diagenesis: examples from Yellowstone National Park and Nevada, U.S.A. *Journal of Sedimentary Research* 75:200–215.

Jahnke, L.L., Stan-Lotter, H., Kato, K., and Hochstein, L.I. (1992) Presence of methyl sterol and bacteriohopanepolyol in an outer-membrane preparation from *Methylococcus capsulatus* (bath). *J Gen Microbiol* 138:1759–1766.

Jahnke, L.L., Eder, W., Huber, R., Hope, J.M., Hinrichs, K.U., Hayes, J.M., Des Marais, D.J., Cady, S.L., and Summons, R.E. (2001) Signature lipids and stable carbon isotope analyses of Octopus Spring hyperthermophilic communities compared with those of *Aquificales* representatives. *Appl Environ Microbiol* 67:5179–5189.

Jahnke, L.L., Embaye, T., Hope, J., Turk, K.A., Van Zuilen, M., Des Marais, D.J., Farmer, J.D., and Summons, R.E. (2004) Lipid biomarker and carbon isotopic signatures for stromatolite-forming, microbial mat communities and *Phormidium* cultures from Yellowstone National Park. *Geobiology* 2:31–47.

Jürgens, U.J. and Weckesser, J. (1986) Polysaccharide covalently linked to the peptidoglycan of the cyanobacterium *Synechocystis* sp. strain PCC6714. *J Bacteriol* 168:568–573.

Kaur, G., Mountain, B.W., and Pancost, R.D. (2008) Microbial membrane lipids in active and inactive sinters from Champagne Pool, New Zealand: elucidating past geothermal chemistry and microbiology. *Org Geochem* 39:1024–1028.

Kaur, G., Mountain, B.W., Hopmans, E.C., and Pancost, R.D. (2011) Preservation of microbial lipids in geothermal sinters. *Astrobiology* 11:259–274.

Kenig, F., Damsté, J.S.S., Kock-van Dalen, A.C., Rupstra, W.I.C., Huc, A.Y., and de Leeuw, J.W. (1995) Occurrence and origin of mono-, di-, and trimethylalkanes in modern and holocene cyanobacterial mats from Abu Dhabi, United Arab Emirates. *Geochim Cosmochim Acta* 59:2999–3015.

Kenyon, C.N. (1972) Fatty acid composition of unicellular strains of blue-green algae. *J Bacteriol* 109:827–834.

Kenyon, C.N. and Gray, A.M. (1974) Preliminary analysis of lipids and fatty acids of green bacteria and *Chloroflexus aurantiacus*. *J Bacteriol* 120:131–138.

Kenyon, C.N., Rippka, R., and Stanier, R.Y. (1972) Fatty acid composition and physiological properties of some filamentous blue-green algae. *Arch Mikrobiol* 83:216–236.

Klatt, C.G., Bryant, D.A., and Ward, D.M. (2007) Comparative genomics provides evidence for the 3-hydroxypropionate pathway in filamentous anoxygenic phototrophic bacteria and in hot spring microbial mats. *Environ Microbiol* 9:2067–2078.

Klatt, C.G., Inskeep, W.P., Herrgard, M.J., Jay, Z.J., Rusch, D.B., Tringe, S.G., Parenteau, M.N, Ward, D.M., Boomer, S.M., Bryant, D.A., and Miller, S.R. (2013) Community structure and function of high-temperature chlorophototrophic microbial mats inhabiting diverse geothermal environments. *Front Microbiol* 4, doi:10.3389/fmicb.2013.00106.

Klein, C. (2005) Some Precambrian banded iron formations (BIFs) from around the world: their age, geologic setting, mineralogy, metamorphism, geochemistry, and origin. *Am Mineral* 90:1473–1499.

Knudsen, E., Jantzen, E., Bryn, K., Ormerod, J.G., and Sirevag, R. (1982) Quantitative and structural characteristics of lipids in *Chlorobium* and *Chloroflexus*. *Arch Microbiol* 132:149–154.

Kohnen, M.E.L., Sinninghe Damsté, J.S., and de Leeuw, J.W. (1991) Biases from natural sulfurization in paleoenvironmental reconstruction based on hydrocarbon biomarker distributions. *Nature* 349:775–778.

Konhauser, K.O., Phoenix, V.R., Bottrell S.H., Adams, D.G., and Head, I.M. (2001) Microbial-silica interactions in Icelandic hot spring sinter: possible analogues for some Precambrian siliceous stromatolites. *Sedimentology* 48:415–433.

Köster, J., Volkman, J.K., Rullkötter, S.-B.B.M., Rethmeier, J., and Fischer, U. (1999) Mono-, di- and trimethyl-branched alkanes in cultures of the filamentous cyanobacterium *Calothrix scopulorum*. *Org Geochem* 30:1367–1379.

Lalonde, K., Mucci, A., Ouellet, A., and Gelinas, Y. (2012) Preservation of organic matter in sediments promoted by iron. *Nature* 483:198–200.

Leduc, M., Kasra, R., and Van Heijenoort, J. (1982) Induction and control of the autolytic system of *Escherichia coli*. *J Bacteriol* 152:26–34.

Lipp, J.S., Morono, Y., Inagaki, F., and Hinrichs, K.U. (2008) Significant contribution of archaea to extant biomass in marine subsurface sediments. *Nature* 454:991–994.

Lutz, S.J., Caskey, S.J., Mildenhall, D.D., Browne, P.R.L., and Johnson, S.D. (2002) Dating the sinter deposits in northeastern Dixie Valley, Nevada—the paleoseismic record and implications for the Dixie Valley geothermal system [SGP-TR-171]. In *Proceedings, Twenty-Seventh Workshop on Geothermal Reservoir Engineering,* Stanford University, Stanford, CA.

Madigan, M.T., Jung, D.O., Karr, E.A., Sattley, W.M., Achenbach, L.A., and van der Meer, M.T.J. (2005) Diversity of anoxygenic phototrophs in contrasting extreme environments. In *Geothermal Biology and Geochemistry in Yellowstone National Park,* edited by W.P. Inskeep and T.R.S McDermott, Thermal Biology Institute, Montana State University, Bozeman, MT, pp 203–219.

Marshall, C.P., Love, G.D., Snape, C.E., Hill, A.C., Allwood, A.C., Walter, M.R., Van Kranendonk, M.J., Bowden, S.A., Sylva, S.P., and Summons, R.E. (2007) Structural characterization of kerogen in 3.4 Ga Archaean cherts from the Pilbara Craton, Western Australia. *Precambrian Res* 155:1–23.

Miller, M., Pedersen, J.Z., and Cox, R.P. (1988) Effect of growth temperature on membrane dynamics in a thermophilic cyanobacterium: a spin label study. *Biochim Biophys Acta* 943:501–510.

Mountain, B.W., Benning, L.G., and Boerema, J.A. (2003) Experimental studies on New Zealand hot spring sinters: rates of growth and textural development. *Can J Earth Sci* 40:1643–1667.

Nübel, U., Bateson, M.M., Vandieken, V., Wieland, A., Kuhl, M., and Ward, D.M. (2002) Microscopic examination of distribution and phenotypic properties of phylogenetically diverse *Chloroflexaceae*-related bacteria in hot spring microbial mats. *Appl Environm Microbiol* 68:4593–4603.

Ourisson, G. and Albrecht, P. (1992) Hopanoids 1. Geohopanoids: the most abundant natural products on Earth? *Pure Appl Chem* 51:709–729.

Ourisson, G., Rohmer, M., and Poralla, K. (1987) Prokaryotic hopanoids and other polyterpenoid sterol surrogates. *Annu Rev Microbiol* 41:301–333.

Pancost, R.D., Pressley, S., Coleman, J.M., Benning, L., and Mountain, B.W. (2005) Lipid biomolecules in silica sinters: indicators of microbial biodiversity. *Environ Microbiol* 7:66–77.

Pancost, R.D., Pressley, S., Coleman, J.M., Talbot, H.M., Kelly, S.P., Farrimond, P., Schouten, S., Benning, L., and Mountain, B.W. (2006) Composition and implications of diverse lipids in New Zealand geothermal sinters. *Geobiology* 4:71–92.

Parenteau, M.N. and Cady, S.L. (2010) Microbial biosignatures in iron-mineralized phototrophic mats at Chocolate Pots hot springs, Yellowstone National Park, United States. *Palaios* 25:97–111.

Parfitt, R.L., Van der Gaast, S.J., and Childs, C.W. (1992) A structural model for natural siliceous ferrihydrite. *Clays Clay Miner* 40:675–681.

Phoenix, V.R., Adams, D.G., and Konhauser, K.O. (2000) Cyanobacterial viability during hydrothermal biomineralization. *Chem Geol* 169:329–338.

Phoenix, V.R., Konhauser, K.O., and Ferris, F.G. (2003) Experimental study of iron and silica immobilization by bacteria in mixed Fe–Si systems: implications for microbial silicification in hot springs. *Can J Earth Sci* 40:1669–1678.

Pierson, B.K. and Castenholz, R.W. (1974) A phototrophic gliding filamentous bacterium of hot springs, *Chloroflexus aurantiacus*, gen. and sp. nov. *Arch Microbiol* 100:5–24.

Pierson, B.K. and Parenteau, M.N. (2000) Phototrophs in high iron microbial mats: microstructure of mats in iron-depositing hot springs. *FEMS Microbiol Ecol* 32:181–196.

Pierson, B.K., Parenteau, M.N., and Griffin, B.M. (1999) Phototrophs in high-iron-concentration microbial mats: physiological ecology of phototrophs in an iron-depositing hot spring. *Appl Environ Microbiol* 65:5474–5483.

Pohl, P., Glasl, H., and Wagner, H. (1970) Zur analytik pflanzlicher glyhko- und phospholipoide und ihrer fettsäuren i. Eine neue dünnschichtchromatograhische methode zur trennung pflanzlicher lipoide und quantitativen bestimmung ihrer fettsäure-zusammñsetzung. *J Chromatogr A* 49:488–492.

Rashby, S.E., Sessions, A.L., Summons, R.E., and Newman, D.K. (2007) Biosynthesis of 2-methylbacteriohopanepolyols by an anoxygenic phototroph. *Proc Natl Acad Sci USA* 104: 15099–15104.

Ratledge, C. and Wilkinson, S.G. (1988) *Microbial Lipids,* Academic Press, San Diego, CA.

Rezanka, T., Nedbalová, L., Elster, J., Cajthaml, T., and Sigler, K. (2009) Very-long-chain *iso* an *anteiso* branched fatty acids in *N*-acylphosphatidylethanolamines from a natural cyanobacterial mat of *Calothrix* sp. *Phytochemistry* 70:655–663.

Robinson, N. and Eglinton, G. (1990) Lipid chemistry of Icelandic hot spring microbial mats. *Org Geochem* 15:291–298.

Rohmer, M., Bouvier-Navre, P., and Ourisson, G. (1984) Distribution of hopanoid triterpenes in prokaryotes. *J Gen Microbiol* 130:1137–1150.

Ruff, S.W., Farmer, J.D., Calvin, W.M., Herkenhoff, K.E., Johnson, J.R., Morris, R.V., Rice, M.S., Arvidson, R.E., Bell, J.F., III, Christensen, P.R., and Squyres, S.W. (2011) Characteristics, distribution, origin, and significance of opaline silica observed by the spirit rover in Gusev Crater, Mars. *J Geophys Res* 116, doi:10.1029/2010JE003767.

Sakamoto, T., Los, D.A., Higashi, S., Wada, H., Nishida, I., Ohmori, M., and Murata, N. (1994) Cloning of ω3 desaturase from cyanobacteria and its use in altering the degree of membrane-lipid unsaturation. *Plant Mol Biol* 26:249–263.

Sarrazin, P., Brunner, W., Blake, D., Gailhanou, M., Bish, D.L., Vaniman, D., Chipera, S., Ming, D.W., Steele, A., Midtkandal, I., Amundsen, H.E.F., and Peterson, R. (2008) Field studies of Mars analog materials using a portable XRD/XRF instrument [abstract 2421]. In *39th Lunar and Planetary Science Conference,* Lunar and Planetary Institute, Houston.

Schirmer, A., Rude, M.A., Li, X., Popova, E., and del Cardayre, S.B. (2010) Microbial biosynthesis of alkanes. *Science* 329: 559–562.

Schwertmann, U., Carlson, L., and Fechter, H. (1984) Iron oxide formation in artificial groundwaters. *Schweizerische Zeitschrift fur Hydrologie* 46:185–191.

Shiea, J., Brassell, S.C., and Ward, D.M. (1990) Mid-chain branched mono- and dimethyl alkanes in hot spring cyanobacterial mats: a direct biogenic source for branched alkanes in ancient sediments? *Org Geochem* 15:223–231.

Shiea, J., Brassell, S.C., and Ward, D.M. (1991) Comparative analysis of extractable lipids in hot spring microbial mats and their component photosynthetic bacteria. *Org Geochem* 17:309–319.

Siljeström, S., Lausmaa, J., Sjövall, P., Broman, C., Thiel, V., and Hode, T. (2010) Analysis of hopanes and steranes in single oil-bearing fluid inclusions using time-of-flight secondary ion mass spectrometry (TOF-SIMS). *Geobiology* 8: 37–44.

Sinninghe Damsté, J.S. and de Leeuw, J.W. (1990) Analysis, structure, and geochemical significance of organically bound sulfur in the geosphere: state of the art and future research. In *Advances in Organic Geochemistry 1989,* edited by B. Durand and F.S. Behar, Pergamon, Oxford, pp 1077–1101.

Sinninghe Damsté, J.S., Rijpstra, W.I.C., Kock-van Dalen, A.C., de Leeuw, J.W., and Schenck, P.A. (1989) Quenching of labile functionalized lipids by inorganic sulfur species: evidence for the formation of sedimentary organic sulfur compounds at the early stage of diagenesis. *Geochim Cosmochim Acta* 53:1343–1355.

Sinninghe Damsté, J.S., Rijpstra, W.I.C., Schouten, S., Fuerst, J.A., Jetten, M.S.M., and Strous, M. (2004) The occurence of hopanoids in planctomycetes: implications for the sedimentary biomarker record. *Org Geochem* 35:561–566.

Stasiuk, L.D. (1994) Fluorescence properties of Palaeozoic oil-prone alginite in relation to hydrocarbon generation, Williston Basin, Saskatchewan, Canada. *Marine and Petroleum Geology* 11:219–231.

Summons, R.E., Jahnke, L.L., and Simoneit, B.R.T. (1996) Lipid biomarkers for bacterial ecosystems: studies of cultured organisms, hydrothermal environments, and ancient sediments. In *Evolution of Hydrothermal Ecosystems on Earth (and Mars?),* Ciba Foundation Symposium 202, edited by G.R. Bock and J.A. Goode, John Wiley and Sons, Chichester, UK, pp 174–194.

Summons, R.E., Jahnke, L.L., Hope, J.M., and Logan, G.A. (1999) 2-Methylhopanoids as biomarkers for cyanobacterial oxygenic photosynthesis. *Nature* 400:554–557.

Talbot, H.M., Farrimond, P., Schaeffer, P., and Pancost, R.D. (2005) Bacteriohopanepolyols in hydrothermal vent biogenic silicates. *Org Geochem* 36:663–672.

Talbot, H.M., Summons, R.E., Jahnke, L.L., Cockell, C.S., Rohmer, M., and Farrimond, P. (2008) Cyanobacterial bacteriohopanepolyol signatures from cultures and natural environmental settings. *Org Geochem* 39:232–263.

Tegelaar, E.W., de Leeuw, J.W., Derenne, S., and Largeau, C. (1989) A reappraisal of kerogen formation. *Geochim Cosmochim Acta* 53:3103–3106.

Trouwborst, R.E., Johnston, A., Koch, G., Luther, G.W., and Pierson, B.K. (2007) Biogeochemistry of Fe(II) oxidation in a photosynthetic microbial mat: implications for Precambrian Fe(II) oxidation. *Geochim Cosmochim Acta* 71:4629–4643.

Urrutia, M.M. and Beveridge, T.J. (1993) Mechanism of silicate binding to the bacterial cell wall in *Bacillus subtilis*. *J Bacteriol* 175:1936–1945.

Urrutia, M.M. and Beveridge, T.J. (1994) Formation of fine-grained metal and silicate precipitation on a bacterial surface (*Bacillus subtilis*). *Chem Geol* 116:261–280.

van der Meer, M.T., Schouten, S., Ward, D.M., Geenevasen, J.A., and Sinninghe Damsté, J.S. (1999) All-*cis* hentriaconta-9,15,22-triene in microbial mats formed by the phototrophic prokaryote *Chloroflexus*. *Org Geochem* 30:1585–1587.

van der Meer, M.T., Schouten, S., Hanada, S., Hopmans, E.C., Sinninghe Damsté, J.S., and Ward, D.M. (2002) Alkane-1,2-diol-based glycosides and fatty glycosides and wax esters in *Roseiflexus castenholzii* and hot spring microbial mats. *Arch Microbiol* 178:229–237.

van der Meer, M.T., Schouten, S., Sinninghe Damsté, J.S., de Leeuw, J.W., and Ward, D.M. (2003) Compound-specific isotopic fractionation patterns suggest different carbon metabolisms among *Chloroflexus*-like bacteria in hot-spring microbial mats. *Appl Environ Microbiol* 69:6000–6006.

van der Meer, M.T., Schouten, S., Bateson, M.M., Nübel, U., Wieland, A., Kuhl, M., de Leeuw, J.W., Sinninghe Damsté, J.S., and Ward, D.M. (2005) Diel variations in carbon metabolism by green nonsulfur-like bacteria in alkaline siliceous hot spring microbial mats from Yellowstone National Park. *Appl Environ Microbiol* 71:3978–3986.

van der Meer, M.T., Klatt, C.G., Wood, J., Bryant, D.A., Bateson, M.M., Lammerts, L., Schouten, S., Damste, J.S., Madigan, M.T., and Ward, D.M. (2010) Cultivation and genomic, nutritional, and lipid biomarker characterization of *Roseiflexus* strains closely related to predominant *in situ* populations inhabiting Yellowstone hot spring microbial mats. *J Bacteriol* 192:3033–3042.

Ventura, G.T., Kenig, F., Reddy, C.M., Frysinger, G.S., Nelson, R.K., Van Mooy, B., and Gaines R.B. (2008) Analysis of unresolved complex mixtures of hydrocarbons extracted from Late Archean sediments by comprehensive two-dimensional gas chromatography (GC×GC). *Org Geochem* 39:846–867.

Vestal, R.D. and White, D.C. (1989) Lipid analysis in microbial ecology. Quantitative approaches to the study of microbial communities. *Bioscience* 39:535–541.

Wade, M.L., Agresti, D.G., Wdowiak, T.J., Armendarez, L.P., and Farmer, J.D. (1999) A Mössbauer investigation of iron-rich terrestrial hydrothermal vent systems: lessons for Mars exploration. *J Geophys Res* 104:8489–8507.

Walsh, M.M. and Lowe, D.R. (1985) Filamentous microfossils from the 3,500-Myr old Onverwacht Group, Barberton Mountain Land, South Africa. *Nature* 314:530–532.

Walter, M.R. (1972) A hot spring analog for the depositional environment of Precambrian iron formations of the Lake Superior Region. *Econ Geol* 67:965–980.

Walter, M.R. and Des Marais, D.J. (1993) Preservation of biological information in thermal spring deposits: developing a strategy for the search for a fossil record on Mars. *Icarus* 10: 129–143.

Walter, M.R., Des Marais, D.J., Farmer, J.D., and Hinman, N.W. (1996) Lithofacies and biofacies of mid-Paleozoic thermal spring deposits in the Drummond Basin, Queensland, Australia. *Palaios* 11:497–518.

Ward, D.M., Shiea, J., Zeng, Y.B., Dobson, G., Brassell, S., and Eglinton, G. (1989) Lipid biochemical markers and the composition of microbial mats. In *Microbial Mats: Physiological Ecology of Benthic Microbial Communities,* edited by Y. Cohen and E. Rosenburgs, American Society for Microbiology, Washington, DC, pp 439–454.

Ward, D.M., Panke, S., Kloeppel, K.D., Christ, R., and Fredrickson, H. (1994) Complex polar lipids of a hot spring cyanobacterial mat and its cultivated inhabitants. *Appl Environ Microbiol* 60:3358–3367.

Ward, D.M., Ferris, M.J., Nold, S.C., and Bateson, M.M. (1998) A natural view of microbial biodiversity within hot spring cyanobacterial mat communities. *Microbiol Mol Biol Rev* 62:1353–1370.

Warren, L.A. and Ferris, F.G. (1998) Continuum between sorption and precipitation of Fe(III) on bacterial cell surfaces. *Environ Sci Technol* 32:2331–2337.

White, D.C., Davis, W.M., Nickels, J.S., King, J.D., and Bobbie, R.J. (1979) Determination of the sedimentary microbial biomass by extractable lipid phosphate. *Oecologia* 40:51–62.

White, D.C., Meadows, P., Eglinton, G., and Coleman, M.L. (1993) *In situ* measurement of microbial biomass, community structure, and nutritional status. *Philos Trans Phys Sci Eng* 344:59–67.

White, D.C., Pinkart, H.C., and Ringelberg, D.B. (1997) Biomass measurement: biochemical approaches. In *Manual of Environmental Microbiology,* edited by C.J. Hursts, ASM Press, Washington, DC, pp 91–101.

White, D.E., Hutchinson, R.A., and Keith, T.E.C. (1988) *The Geology and Remarkable Thermal Activity of Norris Geyser Basin, Yellowstone National Park, Wyoming,* U.S. Geological Survey Professional Paper 1456, U.S. Geological Survey, Denver, CO.

Yamamoto, K., Shibahara, A., Nakayama, T., and Kajimoto, G. (1991) Determination of double-bond positions in methylene-interrupted dienoic fatty acids by GC-MS as their dimethyl disulfide adducts. *Chem Phys Lipids* 60:39–50.

Zeikus, J.G., Ben-Bassat, A., and Hegge, P.W. (1980) Microbiology of methanogenesis in thermal, volcanic environments. *J Bacteriol* 143:432–440.

Zeng, Y.B., Ward, D.M., Brassell, S.C., and Eglinton, G. (1992) Lipid compositions of Yellowstone (Wyoming, USA) cyanobacterial and *Chloroflexus* mats. *Chem Geol* 95:327–345.

Zhao, J., Huggins, F.E., Feng, Z., and Huffman, G.P. (1994) Ferrihydrite: surface structure and its effects on phase transformations. *Clays Clay Miner* 42:737–746.

Address correspondence to:
Mary N. Parenteau
NASA Ames Research Center
Exobiology Branch
M/S 239-4
Moffett Field, CA 94035

E-mail: Mary.N.Parenteau@nasa.gov

Submitted 13 November 2013
Accepted 4 April 2014